

Characterization and Evolution of Tetrameric Photosystem I from the Thermophilic Cyanobacterium *Chroococcidiopsis* sp TS-821

Meng Li,^{a,b} Dmitry A. Semchonok,^c Egbert J. Boekema,^c and Barry D. Bruce^{a,b,d,e,1}

^aDepartment of Biochemistry, Cellular, and Molecular Biology, University of Tennessee, Knoxville, Tennessee 37996

^bThe Brederes Center for Interdisciplinary Research and Graduate Education, University of Tennessee, Knoxville, Tennessee 37996

^cDepartment of Electron Microscopy, Groningen Biomolecular Sciences and Biotechnology Institute, University of Groningen, 9747 AG Groningen, The Netherlands

^dDepartment of Microbiology, University of Tennessee, Knoxville, Tennessee 37996

^eSustainable Energy and Education Research Center, University of Tennessee, Knoxville, Tennessee 37996

ORCID ID: 0000-0002-4045-9815 (B.D.B.)

Photosystem I (PSI) is a reaction center associated with oxygenic photosynthesis. Unlike the monomeric reaction centers in green and purple bacteria, PSI forms trimeric complexes in most cyanobacteria with a 3-fold rotational symmetry that is primarily stabilized via adjacent PsaL subunits; however, in plants/algae, PSI is monomeric. In this study, we discovered a tetrameric form of PSI in the thermophilic cyanobacterium *Chroococcidiopsis* sp TS-821 (TS-821). In TS-821, PSI forms tetrameric and dimeric species. We investigated these species by Blue Native PAGE, Suc density gradient centrifugation, 77K fluorescence, circular dichroism, and single-particle analysis. Transmission electron microscopy analysis of native membranes confirms the presence of the tetrameric PSI structure prior to detergent solubilization. To investigate why TS-821 forms tetramers instead of trimers, we cloned and analyzed its *psaL* gene. Interestingly, this gene product contains a short insert between the second and third predicted transmembrane helices. Phylogenetic analysis based on PsaL protein sequences shows that TS-821 is closely related to heterocyst-forming cyanobacteria, some of which also have a tetrameric form of PSI. These results are discussed in light of chloroplast evolution, and we propose that PSI evolved stepwise from a trimeric form to tetrameric oligomer en route to becoming monomeric in plants/algae.

INTRODUCTION

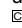
Photosynthetic reaction centers are chlorophyll pigment-protein complexes capable of converting light energy into a stable charge separation. In oxygenic photosynthesis, photosystem II (PSII) and photosystem I (PSI) work in series to couple the splitting of water with the reduction of ferredoxin (Nelson and Yocum, 2006). Whereas PSII has evolved to have a strong oxidizing potential, PSI has evolved to have a low potential acceptor that is capable of reducing NADP⁺ via the soluble Fe/S protein ferredoxin. Interestingly, unlike the nonoxygenic, monomeric bacterial reaction centers, photosynthetic reaction centers in oxygenic organisms are found as monomers (plant PSI), dimers (all PSII), or trimers (cyanobacterial PSI). Cyanobacterial PSI trimers have been reported in many published works (Boekema et al., 1987, 2001; Almog et al., 1991; Kruij et al., 1993, 1994, 1997; Tsiotis et al., 1995; Garczarek et al.,

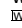
1998; Tucker and Sherman, 2000; Mangels et al., 2002; Bibby et al., 2003; Brecht et al., 2012), and the only existing crystal structure of a cyanobacterial PSI, from *Thermosynechococcus elongatus* BP-1 (Jordan et al., 2001), suggests that cyanobacteria PSI preferentially forms a trimer. Although there have been reports of trimeric forms of PSI in plants (Heinemeyer et al., 2004; Kouril et al., 2005), it is now widely accepted that plant PSI forms only monomeric complexes (Kitmitto et al., 1998; Kouril et al., 2005). Furthermore, it is known that PSI is a monomer in green and red algae (Gardian et al., 2007) as well as in diatoms (Veith and Büchel, 2007).

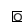
Cyanobacterial PSI trimers have been reported in almost every subclass of cyanobacteria. The most well-characterized PSI trimers are from *Synechocystis*, *Synechococcus*, and *Thermosynechococcus*, and the PSI subunit PsaL is needed for PSI trimerization in these cyanobacteria (Chitnis et al., 1993; Schluchter et al., 1996; Aspinwall et al., 2004). In contrast, plant PSI is monomeric in the presence of PsaL, possibly due to interaction with the PsaH subunit, which is not found in cyanobacteria (Ben-Shem et al., 2004; Nelson and Ben-Shem, 2005; Amunts and Nelson, 2008). However, both PSI tetramer and dimer were reported in the heterocyst-forming cyanobacterium *Nostoc* sp PCC 7120 (Watanabe et al., 2011, 2014). A similar tetrameric PSI was also observed in the glaucophyte alga *Cyanophora paradoxa*, using Blue Native PAGE (BN-PAGE) and Suc density gradient centrifugation (SDGC), but was not characterized in detail (Watanabe et al., 2011).

¹ Address correspondence to bbruce@utk.edu.

The author responsible for distribution of materials integral to the findings presented in this article in accordance with the policy described in the Instructions for Authors (www.plantcell.org) is: Barry D. Bruce (bbruce@utk.edu).

 Some figures in this article are displayed in color online but in black and white in the print edition.

 Online version contains Web-only data.

 Articles can be viewed online without a subscription.
www.plantcell.org/cgi/doi/10.1105/tpc.113.120782

In this study, we identified a third organism, the unicellular cyanobacterium *Chroococcidiopsis* sp TS-821 (TS-821), that contains tetrameric PSI complex. TS-821 is a thermophilic cyanobacterium isolated from a hot spring in Thailand (Hayashi et al., 1994). It was originally identified as a member of the *Chroococcidiopsis* genus according to the physiological and morphological properties described by Stainer and Waterbury (Waterbury and Stanier, 1978). *Chroococcidiopsis* is classified as a class II cyanobacterium because of its 'multi-fission' property, but a recent classification study based on 16S rRNA sequences showed that *Chroococcidiopsis* is a close relative to heterocyst-forming cyanobacteria (Fewer et al., 2002). Thus, the prior classification of *Chroococcidiopsis* may require reconsideration. TS-821 and other related cyanobacteria are remarkable thermophilic cyanobacteria capable of surviving various extreme environments (Hayashi et al., 1994). This extreme environmental tolerance and the ability to grow to high cellular density (Ishida et al., 1997) makes TS-821 an attractive source for large-scale production of thermostable photosynthetic complexes.

In TS-821, PSI forms tetrameric and dimeric species, which we have characterized in this study using BN-PAGE, SDGC, 77K fluorescence, circular dichroism (CD), analytical ultracentrifugation (AUC), electron microscopy (EM), and single-particle analysis. To investigate why TS-821 forms tetramers/dimers instead of trimers, the *psaL* gene in TS-821 was cloned and analyzed, revealing that the gene product contains a short insert between the second and third predicted trans-membrane helices. Furthermore, phylogenetic analysis based on PsaL protein sequences revealed that TS-821 is closely related to heterocyst-forming cyanobacteria, some of which also have a tetrameric form of PSI.

The evolutionary process by which PSI evolved from a monomeric Type I reaction center in green bacteria into a trimeric complex found in most cyanobacteria is poorly understood (Amunts and Nelson, 2008). Neither the mechanism nor evolutionary pressure that drove the cyanobacterial trimeric form back to a monomeric form in plants and algae has been determined. However, our work indicates that structural changes in PsaL may be a widespread evolutionary event and provides additional insight about PSI evolution from cyanobacteria to chloroplasts. Additionally, the significance of PSI tetramer in PSI evolution and endosymbiotic origin of chloroplasts is discussed.

RESULTS

Native Organization of TS-821 Photosystems

The robust and highly efficient nature of PSI (Amunts and Nelson, 2009) makes it very attractive for solar energy applications such as hydrogen production and photovoltaics (Mukherjee et al., 2011; LeBlanc et al., 2012; Merishin et al., 2012). Therefore, we sought to isolate and characterize PSI from TS-821 for potential utilization in these applications. To identify the pigment-protein complexes in the thylakoids of TS-821, we used BN-PAGE as a rapid method for identification with a minimum potential for disruption or denaturation (Schägger and von Jagow,

1991). TS-821 thylakoid membranes were solubilized in different concentrations of detergent dodecyl-maltoside (DDM) and analyzed via BN-PAGE. A similar analysis was performed on solubilized thylakoid membranes from the well-characterized thermophilic cyanobacteria *T. elongatus* as a control (Figure 1A). When the thylakoids were solubilized in low DDM concentrations (0.6 to 1.0% w/v), three major green bands and six other faint bands were observed. At a higher detergent concentration, the top green band disappeared, while the middle major green band increased. This result suggests a possible interconversion; however, in agreement with previous studies (Watanabe et al., 2009, 2011), a similar solubilization of the *T. elongatus* thylakoids revealed predominantly PSI trimer, PSII dimer, and PSII monomer by BN-PAGE. The PSI trimer was smaller than the largest green band observed in TS-821 and was not affected by increasing the detergent concentration used for solubilization. Using the actual molecular weights of the *T. elongatus* photosystems (PSII monomer, 350 kD; PSII dimer, 700 kD; PSI trimer, 1068 kD) (Jordan et al., 2001; Umena et al., 2011) as sizing standards in this gel system, the apparent molecular masses of the three large green bands in TS-821 were ~400, ~800, and ~1600 kD (Supplemental Figure 1). These values suggest a size distribution for monomer, dimer, and tetramer forms of PSI, respectively. Furthermore, there is no prominent band corresponding to the trimer as was observed in the membranes from *T. elongatus*.

To further characterize and confirm the identity of each of the green bands observed by BN-PAGE, a second dimensional analysis using SDS-PAGE was performed. The BN-PAGE was repeated using 1.0% DDM solubilized thylakoid membranes (Figure 1B). Individual TS-821 green bands were carefully excised from the BN-PAGE and solubilized in SDS-PAGE sample buffer (Schägger, 2006) and subsequently analyzed using SDS-PAGE with silver stain. For comparison, a similar treatment was applied to solubilized thylakoid membranes of *T. elongatus* (Figure 1C). The identity of the green bands corresponding to PSI and PSII was confirmed by the presence of characteristic subunit bands (PsaA/PsaB, PsaD, PsaF, D1/D2, CP47, and CP43) in the silver-stained SDS-PAGE gel. According to the individual subunit composition and apparent molecular masses of the different green bands, the oligomeric forms were identified, as indicated at the bottom of each lane. This analysis verified that the three large green bands corresponded to PSI, and their native molecular masses indicate that they exist natively in monomeric, dimeric, and tetrameric forms. Monomeric and dimeric PSII are identified in the remaining green bands.

PSI Tetramer Isolation

To confirm the presence of PSI tetramer observed by BN-PAGE, a two-step SDGC fractionation similar to what has been reported for isolation of the *T. elongatus* PSI trimer was developed (Iwuchukwu et al., 2010). After the first SDGC, the tetramer was readily detected and collected (Figure 2A). The isolated PSI tetramer was analyzed by BN-PAGE (Figure 2C), which showed some contaminating proteins. This crude tetramer was loaded on a second Suc gradient after dialysis and concentration. Four distinct green bands were observed following centrifugation,

suggesting that the tetrameric PSI can disassemble into monomer and dimer, while the trimer may be from the first SDGC which did not separate the trimer from tetramer (Figure 2B). The oligomeric statuses of these four bands were confirmed by BN-PAGE (Figure 2C). The SDS-PAGE analysis of all four green bands from the second SDGC (Supplemental Figure 2A) confirms that they are all TS-821 PSI complexes in different oligomeric states, possibly monomer, dimer, trimer, and tetramer.

Transmission Electron Microscopy of Isolated PSI Particles

Upon isolation of the resolved tetrameric PSI particles by SDGC, their organization was investigated by scanning transmission electron microscopy (STEM) and transmission electron microscopy

(TEM). Unlike the organization of the PSI trimer from *T. elongatus* (Figure 2D), the tetramer from TS-821 clearly reveals each of the four monomers organized in a somewhat “four-leaf clover” arrangement (Figure 2F). In comparison, the *T. elongatus* monomeric PSI isolated from dissociated PSI trimer tend to form chain structures or amorphous structures, as shown in Figure 2E. This result suggests that the TS-821 tetrameric PSI unlikely resulted from monomeric PSI aggregation.

Single-Particle Analysis of TS-821 PSI

Upon isolation and staining with uranyl acetate, we performed a TEM analysis of the single particles. EM showed the presence of exclusively tetrameric PSI particles in different orientations on

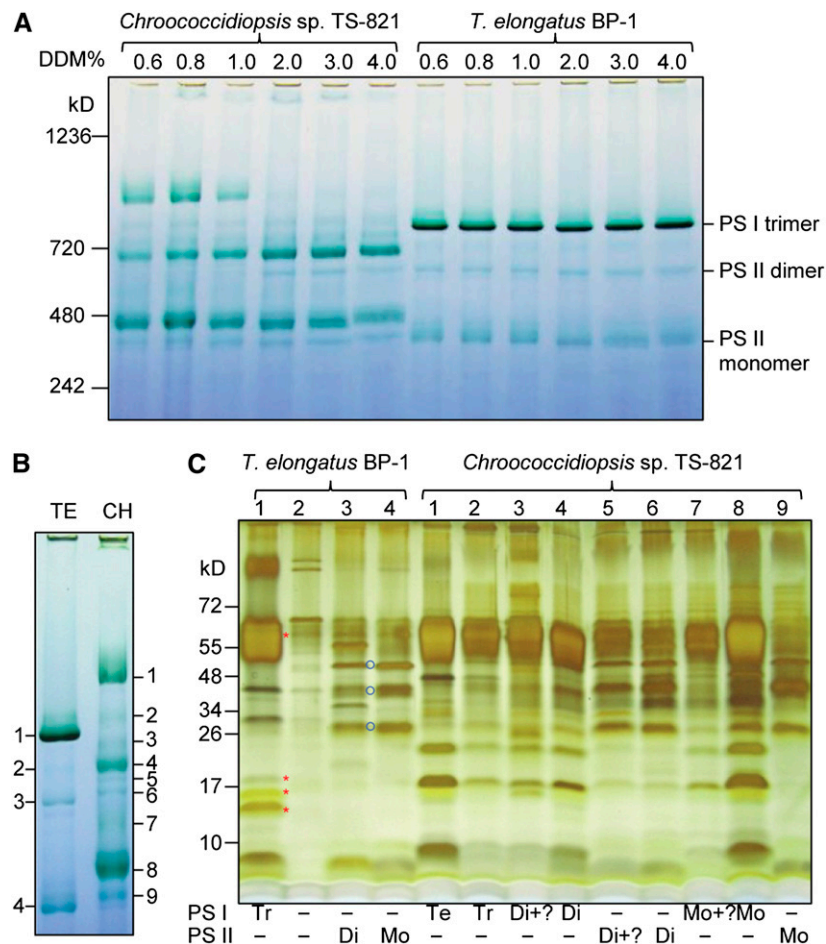


Figure 1. Thylakoid Membrane Solubilization and Photosystem Identification.

(A) BN-PAGE of solubilized thylakoid membranes from *Chroococcidiopsis* sp strain TS-821 (CH) and *T. elongatus* BP-1 (TE). Thylakoid membranes containing 0.2 mg/mL chlorophyll were solubilized in different concentrations of the detergent DDM and loaded on a 4 to 16% BN-PAGE gel. The numbers above each lane indicate the concentration of DDM (w/v %). Soluble protein marker positions are indicated on left.

(B) BN-PAGE of 1% DDM solubilized thylakoid membranes (0.2 mg/mL chlorophyll) from TE and CH. Visible bands before staining, as labeled, were cut out and denatured in SDS-PAGE sample solubilization buffer for subsequent SDS-PAGE.

(C) SDS-PAGE of proteins from BN-PAGE. Characteristic subunit bands for PSI (asterisks) and PSII (circles) from TE are used to identify photosystems in CH. The identification results are shown underneath each lane with the inference of monomer (Mo), dimer (Di), trimer (Tr), tetramer (Te), and uncertainty (?) indicated. Silver stain was used to visualize SDS-PAGE bands.

[See online article for color version of this figure.]

the carbon support film. Classification of projections showed that ~5000 projections were more or less representing nontilted views (Figure 3A), showing a 2-fold symmetry. A 2-fold rotational symmetry was also imposed on the 2D after processing (Figure 3B). The majority of 25,000 particles were substantially tilted on the support film (Figure 3C). The maps indicate that although the complex is clearly composed from four PSI monomers, the association of these monomers is in such a way that it creates a pseudo-tetramer with just 2-fold rotation symmetry, which is compatible to a situation in which two PSI dimers associate into a tetramer. The averaged image of biochemically isolated TS-821 PSI dimers (Figure 3D) is also consistent with the PSI tetramer being composed of a dimer of dimers, yet the precise orientation and assembly interface is not clear from this analysis.

TEM of Native Membranes Reveal PSI Tetramers

To investigate if PSI tetramer exists in native thylakoid membrane, the TEM images of TS-821 thylakoids were acquired (Figure 4A). The particles with right size according to isolated PSI tetramer (Figure 3) were selected and analyzed (Figure 4B). The averaged image (Figures 4C and 4D) of those particles showed high similarity to isolated PSI tetramer. This indicates the presence of PSI tetramer in the native thylakoid membrane of TS-821.

Characterization of Tetrameric PSI

Both BN-PAGE and SDGC showed that TS-821 PSI exists as a tetramer, with significant amounts of dimeric and monomeric forms and very little trimer. The dimeric forms could reflect intermediates during tetramer assembly or possibly be the result of disassembly due to detergent disruption. To test the latter possibility, the purified tetramer was treated with increasing concentration of DDM, which resulted in decreased amount of tetramer and increased amount of dimer and monomer (Figure 5A). Quantification of the different oligomeric forms (Figure 5B) suggested that the tetramer disassembles into the dimer directly, which appears quite stable since it only partially disassembled into the monomer. This can be explained by the structural features of TS-821 PSI tetramer and dimer: A tetrameric PSI has two PSI dimers associated together with inter-dimer gaps, while the PSI dimer is composed of two tightly tethered PSI monomers (Figure 3). Interestingly, the amount of trimer remained low and did not change as a function of DDM concentration. This correlation would suggest that the trimeric form is not only a minor component in thylakoids based on BN-PAGE but is unable to form a stable intermediate or undergo interconversion with the other oligomeric forms.

The different oligomeric forms of many cyanobacterial PSI display altered emission peaks in low temperature fluorescence (77K). The *Spirulina platensis* and *T. elongatus* PSI trimer have an emission peak at ~730 nm with the monomer emission blue-shifted to ~715 to 725 nm (Karapetyan et al., 1997; El-Mohsnawy et al., 2010). The 77K fluorescence showed that TS-821 PSI monomer, dimer, and tetramer share a common emission peak at 715 nm (Figure 6A); however, similar analysis of the isolated monomers and trimers from *T. elongatus* display

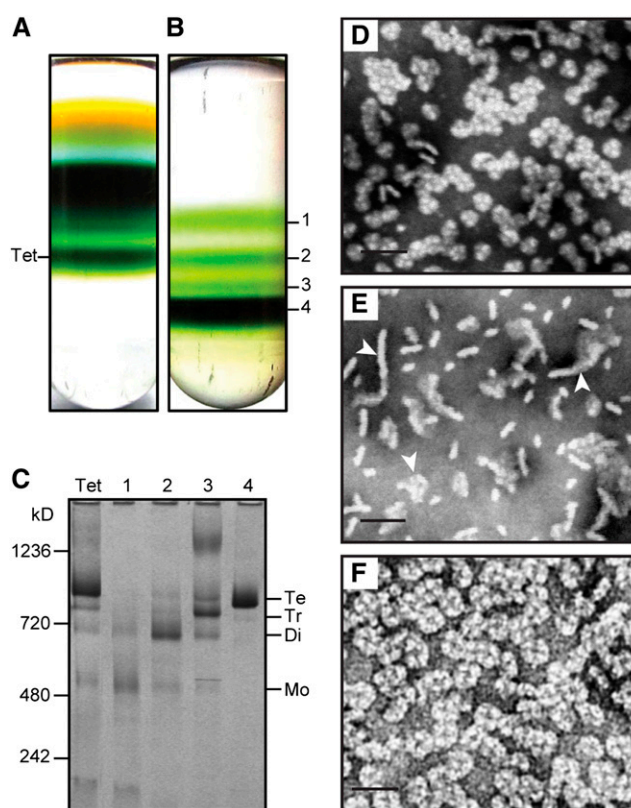


Figure 2. Isolation of TS-821 PSI Tetramer and Proof of Tetramer presence.

(A) PSI tetramer (Tet) isolation from solubilized TS-821 thylakoid membrane using Suc gradient ultracentrifugation.

(B) PSI separation in Suc gradient after second ultracentrifugation. Tetramer isolated from thylakoid membranes was dialyzed and loaded on a second Suc gradient to further purify the tetramer. Four bands as labeled were isolated and loaded on BN-PAGE for analysis.

(C) BN-PAGE analysis of PSI oligomers isolated from Suc gradient ultracentrifugation. Image was taken after Coomassie blue staining.

(D) STEM image of isolated *T. elongatus* PSI trimer.

(E) STEM image of isolated *T. elongatus* PSI monomer. Arrow heads point to examples of monomeric PSI aggregation.

(F) TEM image of isolated TS-821 PSI tetramer. Bars = 50 nm.

[See online article for color version of this figure.]

different peak emissions, in agreement with previously published values of <725 and ~730 nm, respectively (Figure 6A). The blue shift in the 77K fluorescence to the lower value of 715 nm suggests that the chlorophyll emission in all three forms of the TS-821 PSI complex share a similar environment and lack the far red form that is associated with the trimeric form of other cyanobacterial PSI complexes. Consequently, some of the tetrameric chlorophylls could experience a “monomeric-like” environment. Interestingly, the organization of the tetramer as revealed from the single particle analysis reveals a central cavity of low electron density (shown most clearly in Figure 3B). This is contrast to a more uniform density that exists between the individual monomers observed in the TEM of the trimeric structures (Kruip et al., 1997; Bibby et al., 2001). Although we do not

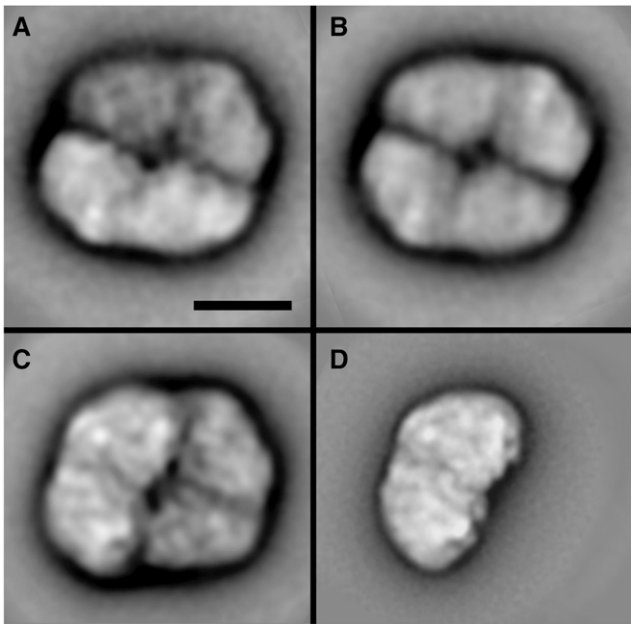


Figure 3. Final Two-dimensional Maps of TS-821 PSI after Single Particle Averaging with Classification.

- (A) Close-to nontilted map of tetramers, best 1024 particles out of 5000.
 (B) Map of frame A, with 2-fold rotational symmetry imposed.
 (C) A typical tilted map of 2048 summed particles from a homogeneous class of in total 10,000 projections.
 (D) Map of biochemically isolated PSI dimer, best 2048 particles out of 8000. Bar = 10 nm.

know the chemical composition of this central cavity, it is clearly different from what was observed in trimeric PSI preps and most likely is filled with lipids and/or detergent molecules. This may provide a similar environment to the far-red chlorophyll molecules as observed in monomeric PSI isolated from native or salt- and heat-treated thylakoid membrane (Karapetyan et al., 1997; El-Mohsnawy et al., 2010). To confirm that the emission characteristics of the isolated TS-821 PSI was not an artifact, we investigated the fluorescence properties of PSI in its native form in the membrane by taking the whole cell emission spectrum at 77K (Figure 6B). The comparison of whole cell emission at 77K and that from isolated PSI reveals a 3-nm blue shift of the emission peak of PSI upon isolation; this 3-nm blue shift is also observed in *T. elongatus* PSI (Figure 6B). This indicates that the TS-821 PSI is present in a tetramer/dimeric/monomeric form in thylakoid membrane, yet does not show any spectral evidence of the red shifted peak characteristic of the trimeric form.

Since BN-PAGE can be influenced by variations in anionic lipid composition and/or variations in binding of the negatively charged dye Coomassie blue, which individually or together could alter electrophoretic mobility, an independent means of assessing the size of the tetramer was needed to confirm the results from BN-PAGE. Therefore, AUC was performed using velocity sedimentation. This assay allowed the determination of the sedimentation coefficient of the TS-821 PSI tetramer while also allowing direct comparison to the monomer and trimer

forms of *T. elongatus* PSI. The TS-821 PSI tetramer has a sedimentation coefficient value of 28S (Figure 6C). These values contrast with those of the isolated *T. elongatus* PSI trimer and monomer, which are 21S (dashed line in Figure 6C) and 12S, respectively (Iwuchukwu et al., 2010). These AUC results clearly support the identity of the larger species as a tetramer.

To investigate the thermostability of the PSI complex, the decrease in CD signal of the chlorophyll molecules was monitored with respect to increasing temperature. This approach has been shown to differentiate the thermostability of the bulk antenna chlorophyll as well as the special pair associated with P_{700} . This assay can differentiate the thermostability of PSI complexes from mesophilic cyanobacteria and thermophilic cyanobacteria (Iwuchukwu et al., 2010). The CD spectra of *Chroococcidiopsis* PSI tetramer (Supplemental Figure 3) showed a similar pattern to that of *T. elongatus* PSI trimer as described in a previous study (Iwuchukwu et al., 2010). Based on the peak values from antenna chlorophyll (509 to 515 nm) and P_{700} (701 to 707 nm), the denaturing profile was shown in Figure 6D. The curve was fit using Boltzmann sigmoidal distribution, and the estimated T_m values for antenna chlorophyll and P_{700} were 77 and 81°C, respectively (Figure 6D).

To confirm the photochemical activity of the PSI tetramer, we investigated both the photooxidation at 705 nm and its re-reduction using a recombinant cyt c_6 from *T. elongatus* expressed in *Escherichia coli*. The ability of photobleached P_{700} to recover was dependent on the presence of cyt c_6 . As the molar ratio of cyt c_6 /PSI was increased, the rate of re-reduction increased, yet it did not saturate at the highest level (cyt c_6 /PSI = 40) tested (Figure 6E). This suggests that PSI in TS-821 is similar to *T. elongatus* PSI in using c-type cytochrome as its electron donor. A previous study has shown the different light intensity-dependent photooxidation profiles between *T. elongatus* PSI trimer and monomer (Baker et al., 2014). A similar experiment was performed to compare the photooxidation properties among TS-821 PSI monomer, dimer, and tetramer (Figure 6F). In contrast to the significant cooperativity in *T. elongatus* PSI trimer, with a Hill coefficient at 1.4 (Baker et al., 2014), our results showed the Hill coefficients for TS-821 PSI monomer, dimer, and tetramer are 1.15 ± 0.08 , 1.17 ± 0.15 , and 1.26 ± 0.09 . This indicates the PSI tetramer and dimer have very little ability to share excitons from the antennae chlorophyll of adjacent monomers. This suggests that the mode of interaction between the adjacent monomers is very different in the dimeric/tetrameric form of PSI relative to the trimeric forms studied in other cyanobacteria.

Cloning of *psaL* Gene

Based on the crystal structure and gene deletions, PsaL has been reported as important for PSI trimerization in most cyanobacteria, and its absence results in the loss of the trimer (Chitnis et al., 1993; Schluchter et al., 1996; Aspinwall et al., 2004); therefore, it is of interest to compare the PsaL proteins associated with this tetramer with those PsaL proteins from cyanobacteria that form trimers. The PsaL subunit in TS-821 was suspected to be larger, as indicated by comparison of subunits of purified PSI tetramer and purified *T. elongatus* PSI

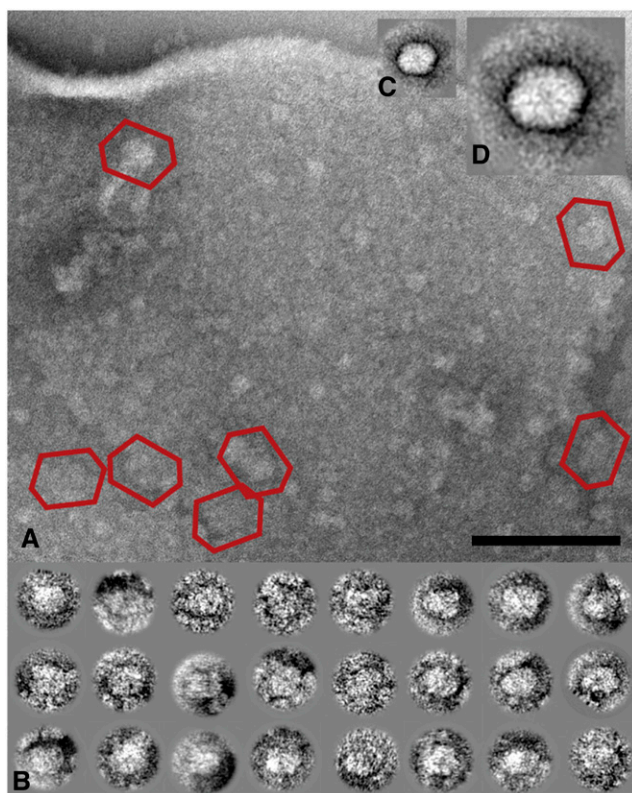


Figure 4. Visualization of Tetrameric PSI Complexes in TS-821 Thylakoid Membrane.

(A) Overview of a part of a double thylakoid membrane depicted in a thick layer of negative stain (2% uranyl acetate). Some visible tetrameric PSI particles are marked by boxes.

(B) A gallery of 24 particles, selected from a series of membranes.

(C) An average of the best 47 projections (out of 150 selected), presented on the same scale as the membrane.

(D) Same average as in (C), magnified 2 \times .

Bar = 100 nm.

[See online article for color version of this figure.]

trimer via SDS-PAGE (Supplemental Figure 2B). A band corresponding to PsaL in *T. elongatus* PSI trimer was not obvious in the tetramer, yet an additional subunit in the tetramer was observed with an apparent molecular mass of ~ 20 kD that was not present in *T. elongatus* PSI trimer. The difference in PsaL gene products may explain the differences in PSI oligomeric state.

In order to identify the possible structural reason for why TS-821 PSI forms tetramers and not trimers, the *psaL* gene from TS-821 was cloned and sequenced. The TS-821 *psaL* gene was cloned initially using a conserved region of the *psaL* gene among heterocyst-forming cyanobacteria as described in Methods. The full-length gene and some flanking sequences were cloned using primers that were designed from the known sequence after partial *psaL* cloning (Figure 7A). Sequencing of this larger genomic fragment allowed the general organization to be determined. Comparison of this genomic structure to other cyanobacteria is shown in Figure 7B. It is clear that the TS-821 *psaL* gene has both *psaF* and *psaJ* genes upstream and the *gmk*

(guanylate kinase) gene downstream, which is similar to the gene arrangement in heterocyst-forming cyanobacteria. Most of the other cyanobacterial *psaL* genes are located adjacent to *psaI*. This PsaL subunit has also been reported to stabilize the PSI trimer (Xu et al., 1995; Schluchter et al., 1996). Interestingly, some heterocyst-forming cyanobacteria as well as close relatives (highlighted species in clade III in Figure 8B), such as *Chroococcidiopsis thermalis* PCC 7203, have two different copies of *psaL*. Moreover, these two genes are also organized differently in their genomes. One organization, mostly having tetrameric PSI, is quite conserved, with *psaL* positioned adjacent to *psaF*, *psaJ*, and *gmk* and the other organization, mostly PSI trimer, has the *psaL* gene placed close to *psaI*, which is often flanked by different, unrelated genes (Figure 7B).

TS-821 *psaL* encodes a 172-amino acid protein with a molecular mass of 18.5 kD. To verify the identity of this *psaL* gene product, liquid chromatography–tandem mass spectrometry (LC-MS/MS) was done using both the intact PSI tetramer complex and the individual subunits upon separation by SDS-

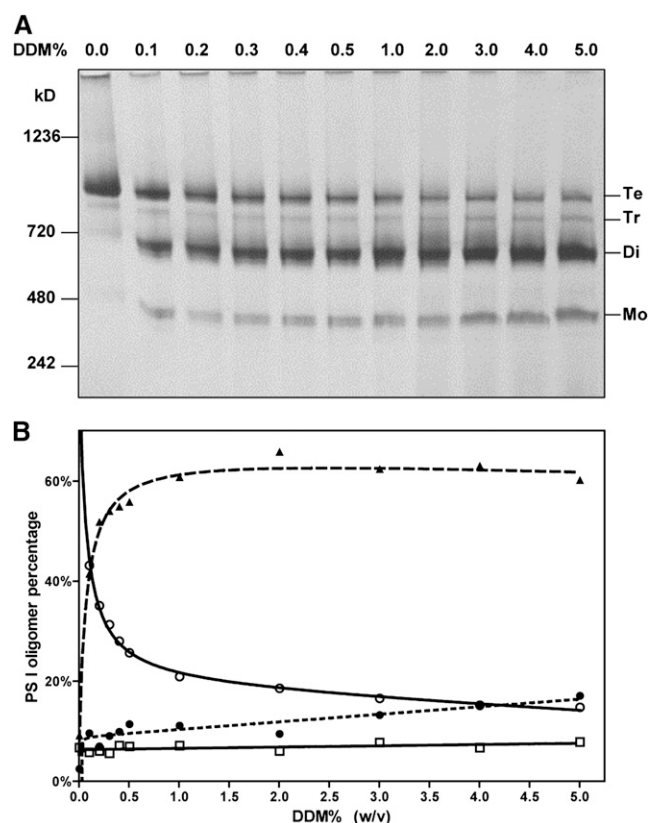


Figure 5. Purified PSI Tetramer Dissociation upon Detergent Treatment.

(A) BN-PAGE analysis of purified PSI tetramer treated using different amounts of the detergent DDM. The final concentrations of DDM (w/v %) are shown on top of each lane. The final concentration of chlorophyll for each lane is 0.15 mg/mL.

(B) Percentages of PSI oligomers under different DDM concentrations. The percentages of TS-821 PSI monomer (filled circle), dimer (filled triangle), trimer (open square), and tetramer (open circle) under different concentrations of DDM are shown.

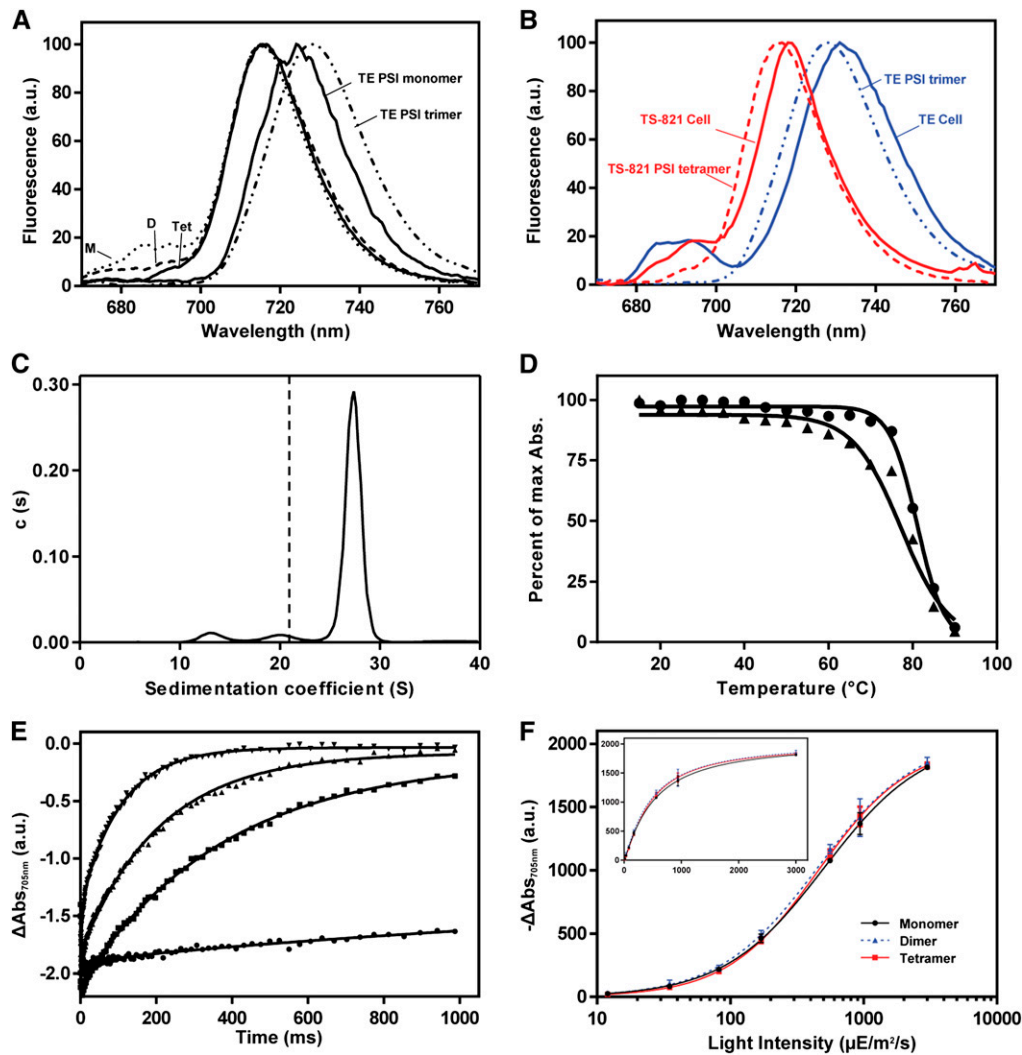


Figure 6. Properties of TS-821 PSI Tetramer.

(A) Low-temperature fluorescence of TS-821 PSI monomer (M), dimer (D), and tetramer (Tet), compared with *T. elongatus* (TE) PSI trimer and monomer. (B) Low-temperature fluorescence of TS-821 whole cell and isolated PSI compared with those from *T. elongatus*.

(C) AUC analysis of TS-821 PSI tetramer. The dashed line denotes previously published S value of the PSI trimer from *T. elongatus* (Iwuchukwu et al., 2010). (D) Thermostability of PSI tetramer inferred from the CD spectra. Triangles indicate the maximum absorbance around 515 nm and circles show those values around 705 nm.

(E) PSI tetramer reduction using *T. elongatus* cytochrome c_6 . Different concentrations of cytochrome were used. Circle, square, triangle, and upside down triangle show the cytochrome c to PSI ratio of 0, 10, 20, and 40, respectively.

(F) Photooxidation of TS-821 PSI monomer, dimer, and tetramer with different light intensities. The same graph with linear light intensity axis is shown in the embedded panel, which shows the saturation of the oxidation.

[See online article for color version of this figure.]

PAGE and gel band excision. This proteomic analysis was conducted using the genomes from closely related cyanobacteria, yet still convincingly showed that the ~20-kD subunit is PsaD and the following smaller band is PsaL (Supplemental Figure 2B and Supplemental Figure 4). Compared with *T. elongatus* and *Synechocystis* PsaL, the PsaL proteins in TS-821, *Chlamydomonas reinhardtii*, and *Arabidopsis thaliana* have shorter C termini but contain longer loop insertions between transmembrane helices 2 and 3 (Figure 8A). Our proteomic results confirms that the TS-821

PsaL is derived from our cloned gene and contains a longer insertion compared with *T. elongatus* and *Synechocystis* PsaL; however, the insertion is still shorter than in green algae and plants (Figure 8A), which have monomeric PSI.

Phylogenetic Analysis

To understand the evolutionary significance between PSI tetramer and PsaL, a phylogenetic tree was built based on PsaL

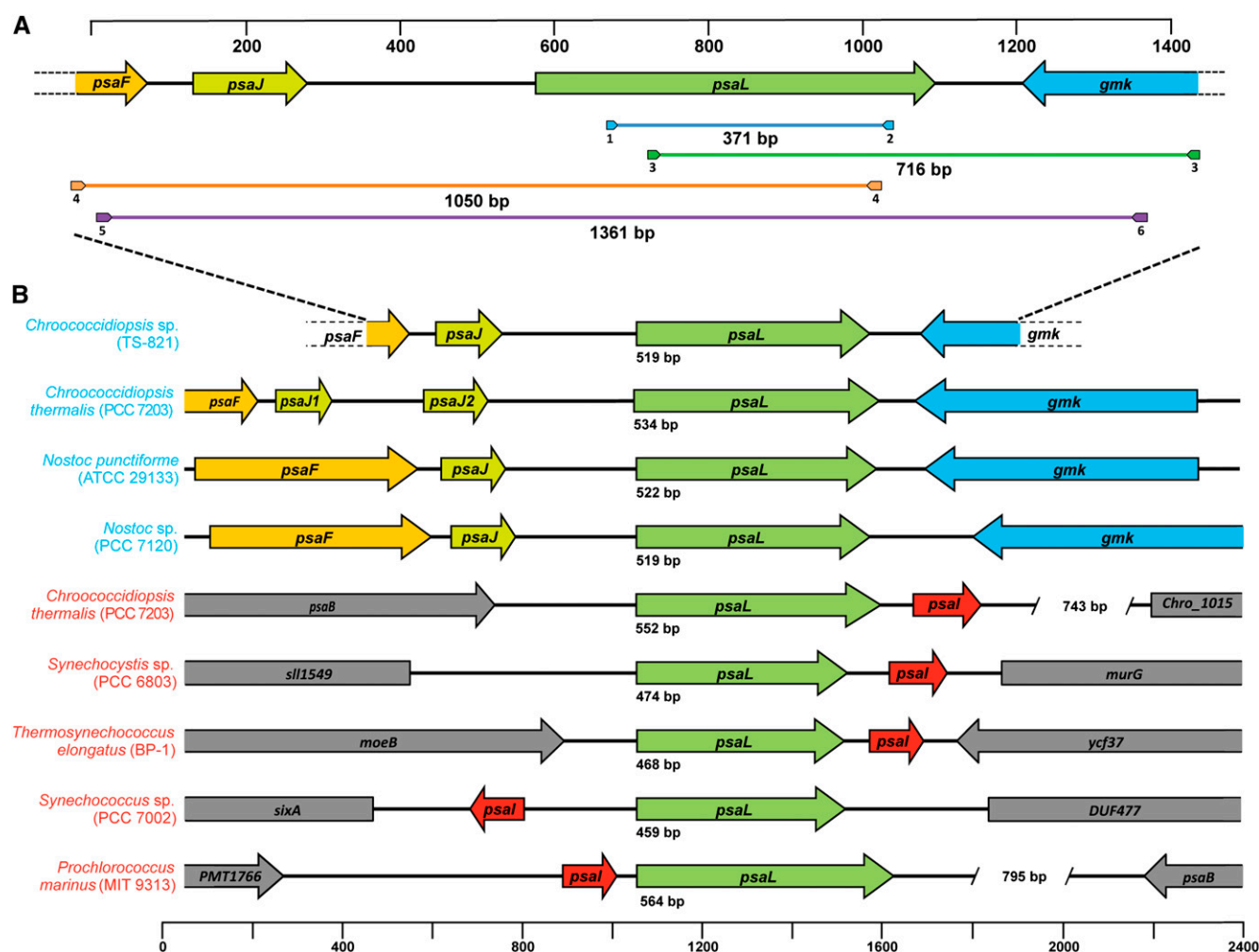


Figure 7. Cloning and Genomic Organization of *psaL* Genes.

(A) Cloning of the TS-821 *psaL* gene was achieved through several steps. First, partial *psaL* sequence was amplified using primers (1 and 2) derived from conserved consensus in heterocyst-forming cyanobacteria *psaL* genes (see Methods for details). With known sequences inside the TS-821 *psaL* gene, primer 3 and primer 4 were designed, both of which independently amplified a flanking region of *psaL*. Primer 5 and primer 6 were designed to confirm the presence of a single *psaL*. The genes were identified using translated DNA sequences.

(B) Cyanobacterial *psaL* genomic locus comparison. Most cyanobacterial *psaL* genes locate either adjacent to *psaF*, *psaJ*, and *gmk* (heterocyst-forming cyanobacteria or related) or adjacent to *psal* (other groups). *psaF*, *psaJ*, *psaL*, *psal*, and *gmk* genes are shown in orange, yellow, green, red, and blue, respectively. Other genes are shown in gray. Rulers are shown separately for **(A)** and **(B)**, in units of base pairs.

protein sequences of cyanobacteria, rhodophyta, chlorophyta, and plants (Figure 8B). The unrooted tree was rerooted using *Gloeobacter* and its close relative as an outside group. Cyanobacteria basically fall into three clades: *Thermosynechococcus*-related clade, *Prochlorococcus*-related clade, and heterocyst-forming cyanobacteria clade (denoted as clades I, II, and III, respectively, in Figure 8B). TS-821 falls in clade III, which indicates its close relationship to heterocyst-forming cyanobacteria. PSI tetramer has only been reported in this cyanobacterial clade (Watanabe et al., 2011, 2014). Many cyanobacteria have two different copies of the *psaL* gene (highlighted in Figure 8B). For instance, some heterocyst-forming cyanobacteria in clade III, such as *Fischerella* sp JSC-11, also have a second *PsaL*-encoding gene

that belongs to the *Thermosynechococcus*-related clade I. It would be interesting to see if PSI in these cyanobacteria forms both a tetramer and a trimer. According to the phylogenetic analysis based on *PsaL* sequences, eukaryotes do not belong to any modern cyanobacterial clade studied, indicating the deep evolutionary origin of eukaryotic *PsaL*, shown as clade V and R for Viridiplantae and Rhodoplantae, respectively (Figure 8B).

DISCUSSION

Using very similar conditions that have been developed for other thermophilic cyanobacteria (Almog et al., 1991; Iwuchukwu

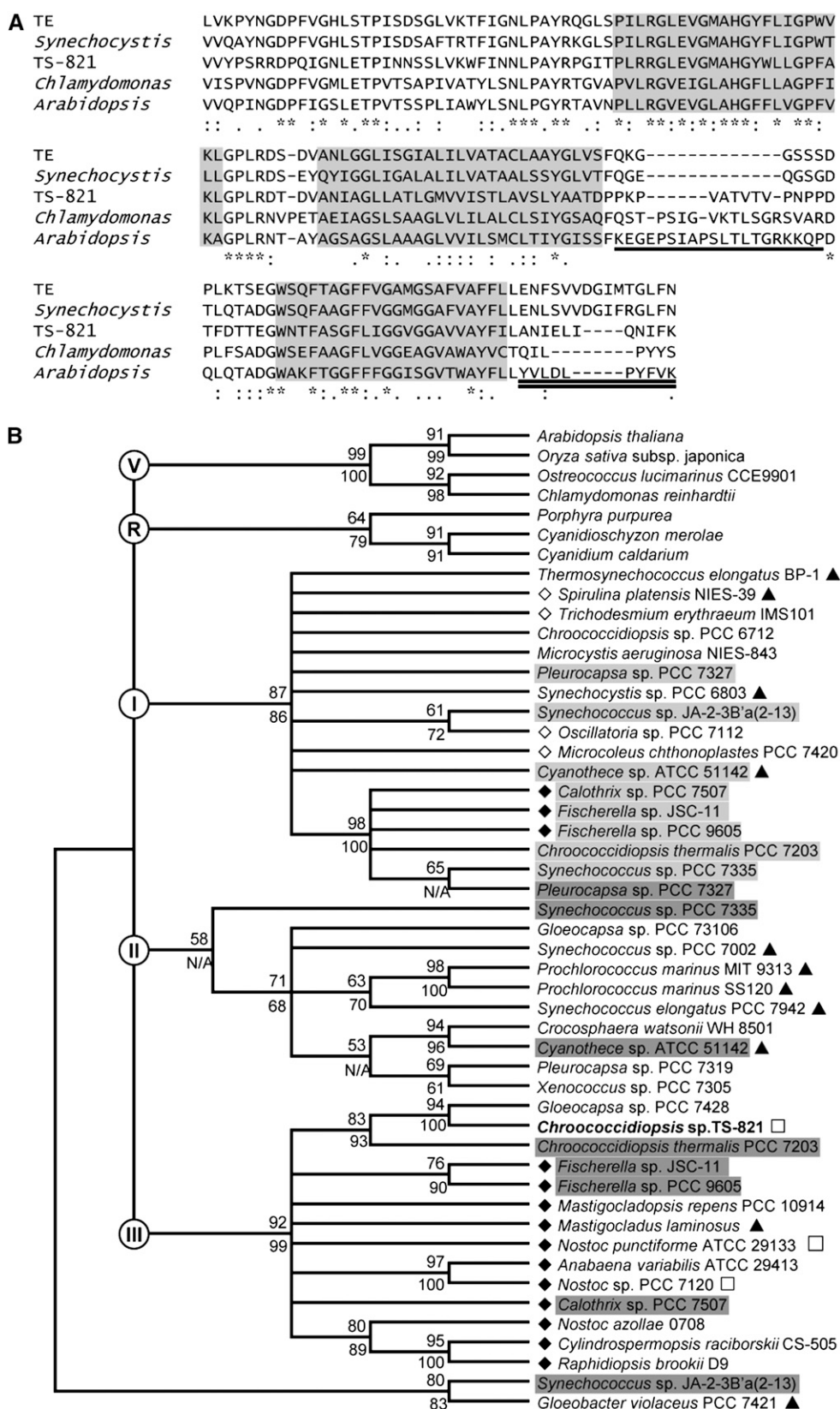


Figure 8. Alignment of Selected PsaL Sequences and Phylogenetic Tree Based on PsaL Protein Sequences.

et al., 2010; Watanabe et al., 2011), we verified the presence of PSI tetramer in TS-821. BN-PAGE and SDS-PAGE analysis of thylakoids showed the majority of TS-821 PSI is present in the membrane as either a tetramer or dimer with a significant amount of monomer (Figure 1). Similar analysis of thylakoids from *T. elongatus* revealed predominantly trimeric form of PSI. Interestingly, the thylakoids of TS-821 show very small amounts of a green band with a similar molecular mass to a PSI trimer (Figure 1B). The presence of multiple forms of PSI suggest that there may be some equilibrium between the monomer, dimer, and tetramer and may suggest a stepwise process of assembly.

The PSI tetramer, with a sedimentation coefficient of 28S (Figure 6F), can be isolated using SDGC for further analysis. The electron micrograph showed the organization of the PSI tetramer comprising four monomers that are somewhat loosely tethered in the center, forming a dimer of dimers (Figures 2F and 3). Noticeably, there is a cavity in the center of the PSI tetramer, not observed in the native membrane, which may harbor some cofactors or lipids that are washed away during preparation. This four-leaf clover structure allows considerably more solvent access to each monomer than what is observed in the relatively tightly organized trimer that has been observed for the *T. elongatus* trimer in this work and others (Iwuchukwu et al., 2010). In addition, careful TEM analysis also rules out the possibility that the larger PSI complex observed was larger due to the association with additional antennae complexes, such as IsiA, as has been observed in some iron-stressed cyanobacteria (Bibby et al., 2001; Kouril et al., 2003, 2005a, 2005b; Ihalainen et al., 2005).

The fact that we observed this tetramer in native membranes prior to detergent solubilization confirms that this tetrameric PSI is not an artifact that results from aggregation on monomers or some other membrane protein complex (Figure 4). A second argument against and artifactual self-assembly is the failure of *T. elongatus* monomers to reassembly into a tetrameric structure following their monomerization (Figure 2E). These monomers form larger aggregates that may result from hydrophobic interactions, similar to what has been observed for plant PSI preparations (Kouril et al., 2005). Analysis of the isolated TS-821 tetramer by BN-PAGE indicates that this high molecular mass species remains even when high levels of detergent are added (5% DDM) (Figure 5), suggesting the tetramer is unlikely an artifact arising from insufficient detergent solubilization. Furthermore, the 77K fluorescence emission spectra of TS-821 whole cell and PSI (Figure 6B) confirm the presence of a dimeric/tetrameric PSI in the thylakoid membrane before isolation and solubilization. This whole-cell measurement plus the TEM data (Figure 4) provide dual evidence that PSI exist as tetramers in

the membrane prior to solubilization. This is also consistent with results from the BN-PAGE of the solubilized thylakoids, which show little PSI with a mobility characteristic of a trimer (Figure 1A).

Due to the novel size and organization of the PSI tetramer, we wanted to further investigate the functional properties of this form of PSI. One of the features of trimeric PSI observed in most cyanobacteria is the presence of a low-temperature, far-red fluorescent species. This species is lost when the complex is denatured, dried, or exposed to high levels of detergent (Kiley et al., 2005). This shift in emission wavelength between the PSI monomer and trimer forms has been observed in various cyanobacteria (Karapetyan et al., 1997; Gobets et al., 2001; El-Mohsawy et al., 2010; Schlodder et al., 2011) with the PSI trimer containing more far-red chlorophylls. It has been observed that in *T. elongatus*, this far-red species is lost or significantly shifted to the blue in the monomeric form (El-Mohsawy et al., 2010). Interestingly, in TS-821, the tetrameric PSI does not contain a prominent far-red fluorescent species. As shown in Figure 6A, the emission spectra of the TS-821 PSI monomer, dimer, and tetramer preparations are nearly the same. According to a previous study, some far-red chlorophylls are located in the interfaces between trimeric PSI monomers (El-Mohsawy et al., 2010). In contrast to the PSI trimers, TS-821 PSI tetramer showed almost no difference from dimer and monomer in low-temperature fluorescence emission. These results suggest a model in which four PSI monomers interact with each other without the involvement of interfacial chlorophylls, which, in contrast, are key components of PSI trimer in *T. elongatus* (Jordan et al., 2001). This model is consistent with the TEM images showing that two PSI monomers assemble at a 180° angle (Figure 3) instead of 120° in PSI trimer as viewed from the stromal or lumen side. Whether the far-red chlorophyll molecules are simply missing in TS-821 or alternatively their emission properties reflect a different chemical environment is not known.

PsaL probably plays an important role in PSI tetramerization in TS-821 as well as in trimerization in other cyanobacteria. Using an alignment of several *psaL* sequences, we were able to design primers to enable the PCR amplification of the TS-821 *psaL* gene. Proteomic analysis identified nine different peptides (covering 37% of the coding sequence, as shown in Supplemental Figure 4), which confirmed that this protein is encoded by the *psaL* gene that we cloned (Figure 7A). Based on this gene sequence and proteomic data, the TS-821 PsaL has a shorter C terminus and a longer insertion between transmembrane helices 2 and 3 than PsaL in *Synechocystis* PCC 6803 and *T. elongatus* (Figure 8A). The distinct features of PsaL in TS-821 tetramer are also present in PsaL from the organisms shown in clade III of Figure 8B, and the sequences

Figure 8. (continued).

(A) Alignment of TS-821 PsaL (TS-821, sequence acquired in this study) with other PsaL sequences from *T. elongatus* BP-1 (TE), *Synechocystis*, *Chlamydomonas*, and *Arabidopsis*. Putative transmembrane helices are highlighted according to the available structure in PDB, 1JB0. The major differences of PsaL sequences among different species are underlined.

(B) Phylogenetic tree of cyanobacteria and plastids based on PsaL protein sequences. Heterocyst-forming cyanobacteria are denoted with filled diamonds, while other filamentous cyanobacteria are labeled with open diamonds. Known PSI trimers (triangles) and tetramers (squares) are labeled at the end of the species' names. Bootstrap values of maximum likelihood and neighbor joining methods are shown at each branch point, upper and lower, respectively. Viridiplantae and Rhodoplantae are denoted as V and R in circles, respectively. Three major cyanobacterial clades are numbered as I, II, and III in circles as well.

are shown in Supplemental Figure 5. Interestingly, this clade includes *Nostoc* sp PCC 7120, which also has been shown to contain a tetrameric form of PSI (Watanabe et al., 2011, 2014). While the longer insertion in TS-821 can make PsaL more flexible for conformational changes, the C terminus of PsaL is believed to stabilize the PSI trimer (Ben-Shem et al., 2004). Collectively, these data suggest that the structural differences in PsaL are responsible for the different oligomeric forms of PSI. To test this hypothesis, we replaced the *psaL* in *Synechocystis* with TS-821 *psaL* using homologous recombination. Although we were successful in replacing this gene, the result was congruent to deleting the entire *psaL* gene because both formed exclusively monomeric PSI lacking PsaL (Supplemental Figure 6). This result suggests that the TS-821 PsaL protein is not expressed or possibly not correctly inserted into the thylakoids. One possible explanation is the different codon usage between *Synechocystis* and TS-821. The TS-821 *psaL* gene has a codon adaptation index of 0.41 versus 0.69 for the native *Synechocystis* *psaL* gene. Although the relationship between the difference of PsaL and tetrameric PSI formation is not proven, numerous studies have shown that PsaL is needed for cyanobacterial PSI monomers to form trimers (Chitnis et al., 1993; Schluchter et al., 1996; Aspinwall et al., 2004). Based on the crystal structure of the *T. elongatus* PSI, it is clear that PsaL forms the organizational center of the trimer (Jordan et al., 2001). In addition to a significant structural role in known PSI trimers, the PsaL sequence has the highest diversity among all the cyanobacterial PSI subunits (Xu et al., 2001). The variation suggests that PsaL differences may explain the diversity in PSI oligomeric forms.

Based on the phylogenetic analysis of the PsaL sequences, we can place TS-821 in clade III, which includes heterocyst-forming cyanobacteria such as *Fischerella* and *Mastigocladus*. However, TS-821 was initially characterized and named according to its morphological and physiological properties (Hayashi et al., 1994). Fewer et al. (2002) reported that *Chroococcidiopsis* is a close relative to heterocyst-forming cyanobacteria based on the cyanobacterial 16S RNA sequences. Our phylogenetic analysis based on PsaL protein sequences (Figure 8B), as well as the genomic organization of the *psaL* gene (Figure 7B), also places TS-821 very close to the heterocyst-forming group of cyanobacteria (Figure 8B). Similar to what we discovered in TS-821, tetrameric PSI has been reported in the heterocyst-forming cyanobacterium *Nostoc* sp PCC 7120 (Watanabe et al., 2011, 2014). The heterocyst PSI in *Nostoc punctiforme* shown on BN-PAGE by Cardona et al. (2009) was interpreted as a tetramer by Watanabe et al. (2011). All of these data, along with our phylogenetic tree, suggest that many if not all of the cyanobacteria in clade III may have tetrameric PSI. Even though PSI trimer in heterocyst-forming cyanobacterium *Mastigocladus laminosus* was reported (Almog et al., 1991), this conclusion does not rule out the possible presence of PSI tetramer in *M. laminosus* because of the different PSI purification method used. Some of the heterocyst-forming cyanobacterial genomes (for example, *Fischerella* and *Calothrix*) contain two *psaL* genes, one of which falls into the trimer-forming clade I and the second aligns with the tetrameric-forming clade III (Figure 8B). It is quite plausible that some cyanobacteria in clade III have

both trimeric and tetrameric PSI either in different cells types or possibly in response to different environmental or physiological conditions. More studies on PSI organization from other heterocyst-forming cyanobacteria are needed to verify this possibility. Unlike the heterocyst-forming cyanobacteria (clade III), almost all other cyanobacteria have trimeric PSI and their PsaL is phylogenetically clustered into either clade I or II (Figure 8B).

The tetrameric PSI, in equilibrium with dimeric and monomeric PSI, can represent a more versatile form of PSI oligomer, compared with tightly associated trimeric PSI. As shown in a previous study, the trimeric PSI has a higher cross section compared with monomeric PSI (Baker et al., 2014), which indicates that trimeric PSI is more efficient in capturing photons, especially under low-light intensity. This agrees with the earlier finding that a *Synechococcus* *psaL* knockout mutant grows slower than the wild type under green light (Schluchter et al., 1996). In contrast to the disadvantage of having a monomeric PSI, the *psaL* mutants of *Synechocystis* and *Synechococcus* showed faster growth rates than wild-type cells when DCMU was added with Glc supplement (Chitnis et al., 1993; Schluchter et al., 1996). These results indicate that having a monomeric PSI is somewhat of an advantage, which is supported by the later observation that both *Synechocystis* and *Synechococcus* downregulate the expression level of PsaL and make more monomeric PSI lacking PsaL under iron deficiency stress (Ivanov et al., 2006). In summary, PSI monomer is favored when cyanobacteria deal with stresses, possibly including high-light intensity. With tetrameric PSI, which is more readily able to dissociate into monomers, TS-821 and other cyanobacteria in clade III can potentially respond to stress or environmental changes faster. Even though the tetrameric PSI does not possess similar high cooperativity to PSI trimer (Baker et al., 2014), the direct attachment of phycobilisome to tetrameric PSI in *Nostoc* sp PCC 7120, in favor of cyclic electron transfer and ATP production in heterocysts, was shown (Watanabe et al., 2014). This indicates that a tetrameric form of PSI may be able to greatly increase its optical cross section in vivo and, hence, higher light energy conversion efficiency (Watanabe et al., 2014). Therefore, the tetrameric form of PSI, attaching to phycobilisome and interconverting with monomeric PSI, may represent a more versatile and advantageous form of PSI in clade III cyanobacteria.

Tetrameric PSI may be the transition form in the evolution from cyanobacterial trimeric PSI to plant monomeric PSI. While most cyanobacterial PSI have been isolated as trimers, PSI from plants is monomeric (Ben-Shem et al., 2003). According to our phylogenetic analysis, PSI can be grouped into three categories: exclusively monomeric (clades R and V), predominantly trimeric (clades I and II), and tetrameric (clade III) (Figure 8B). PSI organization in *Gloeobacter violaceus*, a very primitive cyanobacterium (Mareš et al., 2013), is also a trimer (Mangels et al., 2002), which indicates that trimeric PSI is ancestral to both the tetrameric and monomeric PSI. Besides the discovery of PSI tetramer in TS-821 and *Nostoc*, tetrameric PSI has also been observed in the glaucophyte *C. paradoxa* (Watanabe et al., 2011). Glaucophytes, green algae, and land plants share the same plastid ancestor, while glaucophytes are considered to be more primitive (Keeling, 2004). All of those data combined suggest that PSI evolved from a stable trimer to a metastable

tetramer before becoming exclusively monomeric in plants. A model of this evolutionary transition is shown in Supplemental Figure 7. Some reviews have pointed out that the modification of PsaL C terminus and the emergence of PsaH in plant PSI led to the monomeric form of PSI in plants (Ben-Shem et al., 2004; Nelson and Ben-Shem, 2005; Amunts and Nelson, 2008). In plant PSI monomer, according to the available crystal structure (Amunts et al., 2010), the longer insertion between transmembrane helix 2 and transmembrane helix 3 in PsaL is in close vicinity of PsaH, which indicates their potential interaction that stabilizes the monomeric form of PSI. This insertion, along with short C terminus, is also found in PsaL of tetrameric PSI (Figure 8; Supplemental Figure 5), which further indicates that tetrameric PSI may be an intermediate form during the evolution of the PSI in plants and green algae.

What is the role or position of *Chroococcidiopsis* in the evolutionary transition from cyanobacteria to plastids? Deusch et al. (2008) point out that heterocyst-forming cyanobacteria are the origin of plant plastids by comparing cyanobacterial and plant genomes. However, the placement of heterocyst-forming cyanobacteria as a likely progenitor to the plastid was questioned by Falcón et al. (2010), pointing out the insufficient coverage of the cyanobacterial genome. Instead, Falcón et al. conclude that unicellular nitrogen-fixing cyanobacteria (subsection I) are the closest relative to plastids according to the phylogenetic trees built based on 16S RNA and *rbcl* sequences (Falcón et al., 2010), while other studies support the idea that plastids originated from nitrogen-fixing cyanobacteria (Gupta, 2009; Criscuolo and Gribaldo, 2011; Hackenberg et al., 2011; Kern et al., 2011). One should keep in mind that the phylogenetic trees favoring subsection I being the plastid ancestor are based on one or two sequences. A recent study by Shih et al. (2013) using 25 protein sequences and covering more cyanobacteria genome, tried to explore the common ancestor of the plastid, but this study does not support either of those two positions above. Shih et al. also observed the PsaL-like C terminus extension in some chlorophyll binding proteins (Shih et al., 2013), which indicates that *psaL*-derived gene sequences could have been involved in enabling dynamic interaction with antennae complexes during evolution. At the same time, Gupta (2009) showed the importance and accuracy of using conserved insertions and deletions when studying cyanobacterial phylogenetics. After comparing the sequences of PsaL (shown in Figure 8A) as well as the general genomic organization of *psaL* and its surrounding genes (Figure 7B), it would appear that the nitrogen fixing cyanobacterium TS-821, as well as heterocyst-forming cyanobacteria, has a PsaL that is more closely related to those found in plants and green algae. This structural similarity suggests the possibility that PSI tetramer is evolutionarily closer to the PSI monomer found in most plants and green algae. In addition, the versatility of PSI tetramer may also grant the early endosymbionts high adaptability to constantly change environmental conditions. We speculate that *Chroococcidiopsis* or its close relative is the ancestral origin of plastids, considering the existence of tetrameric PSI in glaucophyte *C. paradoxa*, which supports the conclusion of Deusch et al. (2008).

In summary, we suspect that *Chroococcidiopsis* may be the closest relative to plastids, considering its special characteristics.

Possibly, the tetrameric form of PSI is a common feature shared during cyanobacterial PSI evolution, allowing heterocyst formation and further PSI evolution after endosymbiosis by eukaryotes. To test this hypothesis and find out the ancestral cyanobacteria for plastids, more phylogenomic analyses are needed using more genomic data from some special groups such as *Chroococcidiopsis* and *Cyanophora*.

METHODS

Growth of Cyanobacteria and Isolation of Thylakoid Membrane

Chroococcidiopsis sp TS-821 was cultured in BG-11 medium at 45°C with aeration. Cells were harvested at late log phase. Cell pellets were stored at −20°C or directly washed in buffer A (50 mM MES-NaOH, pH 6.5, 5 mM CaCl₂, and 10 mM MgCl₂) for thylakoid membrane isolation (Watanabe et al., 2009). After pelleting the cell suspension, cell pellets were resuspended in buffer A containing 25% glycerol and homogenized. TS-821 thylakoid membrane isolation was done as described (Watanabe et al., 2009) using a bead beater (MP FastPrep-24) with slight modifications. Thylakoid membranes were precipitated by spinning down at 180,000g for 1 h. The pellets were resuspended in buffer A containing 25% glycerol and stored at −80°C. Chlorophyll concentration was determined as described previously (Iwamura et al., 1970).

Photosystem Analysis Using BN-PAGE and SDS-PAGE

Thylakoid membranes were solubilized in DDM (Glycon) at 25°C for 1.5 h. Insoluble material was removed by centrifuging 180,000g for 5 min at 4°C. Supernatants were taken out for analysis on BN-PAGE of PSI isolation. The 4 to 16% BN-PAGE gels (Invitrogen) were used to analyze solubilized thylakoids or isolated photosystems according to the user manual and references (Schägger and von Jagow, 1991; Wittig et al., 2006). For photosystem identification, 10% acrylamide gel was used as described previously (Schägger, 2006), and silver staining was performed using the fast stain method (Nesterenko et al., 1994). For PSI subunits identification, bands of interest were sliced out after Coomassie Brilliant Blue staining and subsequently treated with trypsin for LC-MS/MS.

Identification of PSI Subunits Using LC-MS/MS

TS-821 PSI subunits bands sliced out from SDS-PAGE gel (Supplemental Figure 2B) were destained at 37°C with 50 mM NH₄HCO₃ pH 8.0 (buffer B) and then dehydrated with 100% acetonitrile. Dried gel pieces were rehydrated with 5 mM 3,3',3''-phosphanetriyltripropionic acid in buffer B to reduce protein disulfide bonds and subsequently with 55 mM iodoacetamide in buffer B to alkylate cysteines. Solution was then replaced with 100% acetonitrile to the dehydrate bands prior to trypsin digestion with 20 µg/mL trypsin in buffer B. For isolated TS-821 PSI tetramer, protein with 0.2 mg/mL chlorophyll was denatured in 7 M urea and 8.3 mM DTT. Treated PSI sample was then diluted using 50 mM Tris and 10 mM CaCl₂ to achieve 1 M urea prior to the addition of 1 µg modified sequencing grade Trypsin Gold (Promega). A six-step multidimensional protein identification technology (Washburn et al., 2001) approach was utilized for enhanced sensitivity over a 12-h analytical timeframe. Peptide extraction was performed as described in a previous study (Olson et al., 2010), and an LTQ-Velos mass spectrometer (Thermo Scientific) was used in this study.

Raw files were transformed into mzML format using MSConvert and searched by MyriMatch (Tabb et al., 2007) software against a compiled database containing putative proteomes of interest (*Gloeocapsa* sp PCC 7428, *Chroococcidiopsis thermalis* PCC 7203, *Thermosynechococcus elongatus* BP-1, and *Nostoc* sp PCC 7120) from UniProt database, putative

TS-821 PsaL sequence, and trypsin. Modifications included static Cys +57 D, dynamic Met +16 D oxidation, and any residue +43 D carbamylation. Results were visualized with IDPicker software and filter parameters required two peptides for protein identifications and set a Q-value of 0.02 or 2% false discovery rate based on matches to decoy sequences.

Suc Density Gradient Isolation of PSI Oligomers

TS-821 thylakoid membrane containing 0.4 mg/mL chlorophyll were solubilized in 0.4% DDM as described above. The solubilized membrane solution was loaded on a 10 to 30% Suc gradient containing buffer A and 0.01% DDM. To isolate pure tetrameric PSI, Suc gradient ultracentrifugation was done twice at 4°C. The first centrifugation was done using an SW-32Ti rotor at 28,000 rpm for 16 h. The bottom green fraction was taken out and dialyzed against buffer A containing 0.01% DDM. Dialyzed PSI tetramer was concentrated using a centrifugal concentrator (Millipore Centrifuplus). Then, the concentrated tetramer was loaded on another 10 to 30% Suc gradient and centrifuged at 28,000 rpm for 24 h. Each green fraction from the second gradient was taken out for dialysis and analysis.

The TS-821 PSI dimer for single particle analysis was made by incubating isolated PSI tetramer with 5% DDM for 1 h at room temperature. Then, the PSI dimer was isolated using SDGC and dialyzed before analysis. The *T. elongatus* PSI monomer was made by adding 0.375% *n*-octyl- β -D-thioglucoiside (Anatrace) into HPLC-purified PSI trimer, with chlorophyll concentration at 0.11 mg/mL, and followed by eighteen heat-freeze cycles inspired by El-Mohsawy et al. (2010) and described in a previous study (Baker et al., 2014).

EM of Isolated PSI Oligomers and TS-821 Thylakoids

Microscopy images of the various PSI preps were acquired using both STEM and TEM. For the STEM, a 5- μ L sample was placed on a freshly glow discharged carbon film supported by a 400 mesh Cu grid (Electron Microscopy Sciences). After 1 min, excess sample was removed and the grid with sample was stained for 1 min with either 0.5% phosphotungstic acid or 1% uranyl. After drying, the sample was imaged with a Zeiss Auriga (Carl Zeiss Microscopy) operating at 30 kV in STEM mode. This allowed direct comparison of the *T. elongatus* trimer, a detergent disrupted *T. elongatus* PSI monomer, and the isolated TS-821 tetramer.

For single-particle analysis, supercomplexes were negatively stained with 2% uranyl acetate for EM carbon-coated copper grids. Imaging and image processing were performed as described in previous studies (Oostergetel et al., 1998; Boekema et al., 1999; Watanabe et al., 2014). For the final class sums, the best 10% of the projections were summed. To visualize TS-821 native thylakoids, TEM was performed. The isolated thylakoid membrane was washed using 0.05% DDM with 0.5 mg/mL chlorophyll for 15 min to remove phycobilisomes. The thylakoid membrane was pelleted by centrifugation at 15,600g for 15 min. The pellets were then washed again in buffer A and spun down. The washed thylakoid membrane was suspended and diluted in buffer A before TEM analysis. TEM images were obtained and analyzed as described previously (Kouřil et al., 2013).

Characterization of PSI Tetramer

To confirm the conversion of PSI tetramer to dimer and monomer, purified TS-821 PSI tetramer in 0.01% DDM with chlorophyll concentration at 0.30 mg/mL was diluted into chlorophyll concentration at 0.15 mg/mL using different concentrations of DDM. After 1.5 h incubation at room temperature, treated PSI tetramer samples were analyzed using BN-PAGE. AUC and 77K fluorescence spectra were analyzed and acquired as described before (Iwuchukwu et al., 2010). CD spectra were scanned from 350 to 760 nm under different temperatures, 15 to 90°C, with 5°C steps and 3-min temperature equilibrations. Thermostability was inferred from graphing the peak value of \sim 510 nm and at \sim 705 nm versus temperature.

For comparison of low temperature fluorescence, we isolated both the monomer and trimer form of PSI from *T. elongatus* BP-1.

PSI P₇₀₀ photooxidation and kinetics of rereduction experiment were performed using a Joliot type spectrometer (JTS-10; BioLogics). *T. elongatus* cyt c₆ expressed in *Escherichia coli* and isolated via IMAC (Iwuchukwu et al., 2010) was used to reduce the photooxidized P₇₀₀ in the presence of 0.1 mM methyl viologen and 0.1 mM ascorbic acid in buffer A containing 0.01% DDM. Kinetics were determined with PSI tetramer at 3 μ g/mL chlorophyll a and cyt c₆/P₇₀₀ ratios were varied from 0, 10, 20, and 40 for comparison. The kinetics was fit using a single exponential decay using GraphPad Prism 6. For light intensity-dependent photooxidation, PSI containing 1 μ g/mL chlorophyll a was photooxidized using actinic light of 10-ms duration. The maximum ΔA_{705} was plotted against light intensity and fit to the allosteric sigmoidal curve.

Genomic DNA Extraction and *psaL* Gene Cloning

TS-821 cells were grown to mid log phase prior to harvesting. The cyanobacterial cells were washed three times using sterile water before DNA extraction. These cells were further washed three times using TE buffer (1 mM EDTA and 10 mM Tris-HCl, pH 7.4) containing 0.6% SDS. Cells were then broken in TE buffer using a beads-beater with 0.1-mm silica beads (MP FastPrep-24), and the following process was described previously by Billi et al. (1998).

According to Fewer et al. (2002), *Chroococcidiopsis* is closely related to heterocyst-forming cyanobacteria. Multiple heterocyst-forming cyanobacterial *psaL* gene sequences (Supplemental Figure 8) and its 5-kb flanking region on both sides were acquired from GenBank and aligned in Megalign (Lasergene DNASTar). This alignment identified highly conserved regions, which were used to amplify the *psaL* gene in TS-821. Primers 5'-GCACCACCAATVCCRC-3' and 5'-GGGAACCTRGAAACVCC-3' were used to amplify an \sim 400-bp fragment within *psaL*. The PCR products were ligated into pGEM T-easy vector (Promega) for sequencing. After acquiring the sequence of the partial *psaL* gene, two other primers based on the known partial sequence, 5'-ATAACCTGCCAGCATATC-3' and 5'-CAAATTAAGAAGCCACTCGC-3', combined with several different putative primers outside *psaL* coding region, were used to obtain the whole *psaL* gene sequence. The result showed that each of the primers independently is capable of amplifying a fragment containing the *psaL* flanking region. Primers based on the sequencing results of flanking regions, 5'-AGATTCTGCT-GATGCGATCG-3' and 5'-GCTTCTGGGGAATTAGTTGC-3', were used to amplify the whole sequence of *psaL* and its flanking regions and verify the presence of single *psaL*. BlastX (<http://blast.ncbi.nlm.nih.gov>) was used to infer the translated protein products. The gene structure is shown in Figure 7A with the primers used for amplification shown. Alignment of the genomic organization of *psaL* with adjacent genes is shown in Figure 7B. Genomic data were taken from NCBI and the JGI Integrated Microbial Genomes site (<https://img.jgi.doe.gov/>).

Phylogenetic Analysis

All other PsaL protein sequences from cyanobacteria, red algae, green algae, and plants were obtained from the Integrated Microbial Genomes (<https://img.jgi.doe.gov/>) and Uniprot (<http://www.uniprot.org/>) databases. For identical sequences, only representative sequences were used for final phylogenetic tree building. The sequences were aligned using ClustalW within MEGA 5 (Tamura et al., 2011) to truncate the first Met, signal peptides in plant and green algae, and N-terminal gap region. The rest of the sequences were submitted to EBI T-Coffee Multiple Sequence alignment (<http://www.ebi.ac.uk/Tools/msa/tcoffee/>) for a better alignment (Notredame et al., 2000). After manually optimizing alignment, phylogenetic analysis with T-Coffee alignment was done with MEGA version 5 (Tamura et al., 2011). The suggested best model, rtREV+G+I+F,

was used for maximum likelihood tree building with five discrete gamma categories, 1000 bootstrap replicates, and 95% site coverage cutoff for gap partial deletion. A neighbor-joining tree was also built using MEGA version 5 using the Poisson model with the same setting as in the maximum likelihood tree. The final tree was a condensed tree with a 50% cutoff.

Construction of *psaL* Mutants in *Synechocystis* sp PCC 6803

Primers 5'-AACCGGTTAGCCCATTCATCAGC-3' and 5'-CCGGGGTAC-CAAGGTCGTCTCC-3', annealing to the flanking region of wild-type *psaL*, were used to clone the wild-type genomic sequence into pCR 2.1-TOPO vector (Invitrogen) for subsequent clone constructions (Supplemental Figure 5A). Site-directed mutagenesis was done to create an *NdeI* restriction site at the wild-type *psaL* start codon. The open reading frame of the kanamycin resistance gene $P_{\text{pccC}}\text{-}km_{\text{r}}^{\text{e}}$ as described in a previous study (Onai et al., 2004) was cloned using primers 5'-GGTTACCCTCGATATTTAGGAG-3' and 5'-GGTAACCTAAAGGGAATGCGT-3', containing *BstEII* restriction sites. The TS-821 *psaL* gene was cloned using primers: 5'-GGTAACCTTACTT-GAAAAATGTTTG-3' and 5'-CATATGGCGCAAGCAATAGATGC-3'. Knock-out mutant of *psaL* (ΔpsaL) and replacing *Synechocystis* *psaL* with TS-821 *psaL* mutant (CH*psaL*) were constructed as shown in Supplemental Figure 5A. Transformation was done using optimum natural transformation conditions as described previously when the cell culture density OD₇₃₀ was ~0.8 (Zang et al., 2007). Kanamycin (60 $\mu\text{g}/\text{mL}$) was used for selection on agar plates and for subsequent liquid culture.

Accession Numbers

Sequence data from this article can be found in the GenBank/EMBL data libraries under accession number KC883473.

Supplemental Data

The following materials are available in the online version of this article.

Supplemental Figure 1. Molecular Weight Estimation of TS-821 PSI Using BN-PAGE

Supplemental Figure 2. SDS-PAGE of TS-821 PSI and *T. elongatus* PSI.

Supplemental Figure 3. CD Spectra of TS-821 PSI Tetramer at Different Temperatures.

Supplemental Figure 4. LC-MS/MS Identification of Subunits in TS-821 PSI Tetramer.

Supplemental Figure 5. *PsaL* Alignment for Phylogenetic Analysis.

Supplemental Figure 6. Genetic Complementation of *Synechocystis* *psaL* Using TS-821 *psaL*.

Supplemental Figure 7. Photosystem I Evolutionary Model.

Supplemental Figure 8. Primer Design for Partial TS-821 *psaL* Gene Cloning.

ACKNOWLEDGMENTS

We thank John Dunlap for assistance with the STEM imaging, Carlee McClintock for assistance with LC-MS/MS, Edward Wright for assistance with AUC, Yuwadee Peerapornpisal from Cheng Mai University for the generous gift of TS-821, and Prakitchai Chotewutmontri for assistance in securing this strain from Cheng Mai University. We thank R. Carter, R. Simmerman, K. Nguyen, Non Chotewutmontri, and R.J. Miltenberger for discussion and critically reading the article. Support has been provided from the Gibson Family Foundation, the Bredeson Center for Interdisciplinary Research and Education, the Tennessee Plant Research Center,

a UTK Professional Development Award, and National Science Foundation support to B.D.B. (DGE-0801470 and EPS-1004083). M.L. has been supported as a CIRE Fellow at University of Tennessee, Knoxville. Work at University of Groningen was supported by the HARVEST Marie Curie Research Training Network (PITN-GA-2009-238017). Travel of B.D.B. to The Netherlands was supported by a Professional Development Award from The Graduate School at UTK.

AUTHOR CONTRIBUTIONS

M.L. and B.D.B. designed the research. M.L. performed the biochemistry research. M.L., E.J.B., and B.D.B. analyzed the data. D.A.S., E.J.B., and M.L. performed the single-particle analysis in Groningen. M.L. and B.D.B. wrote the article.

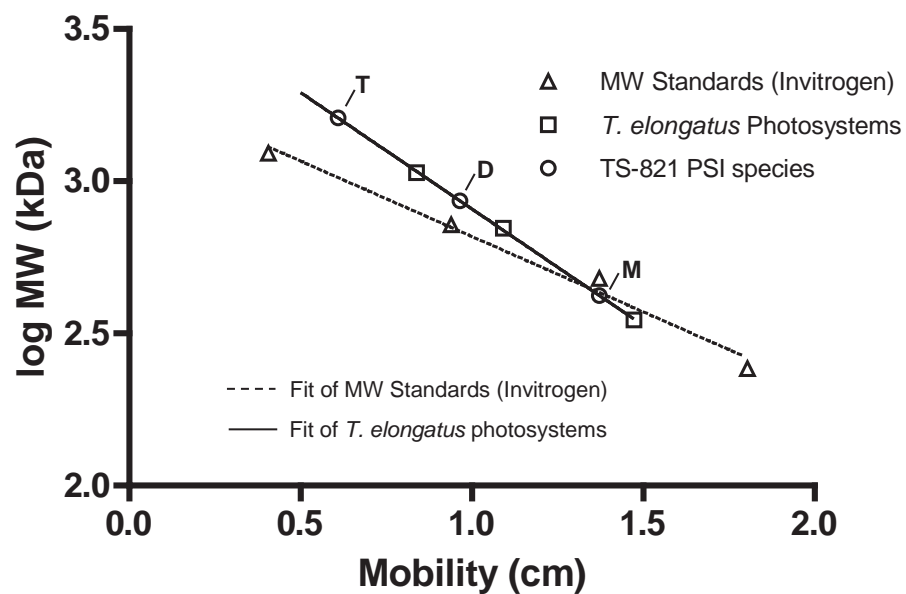
Received November 21, 2013; revised March 9, 2014; accepted March 13, 2014; published March 28, 2014.

REFERENCES

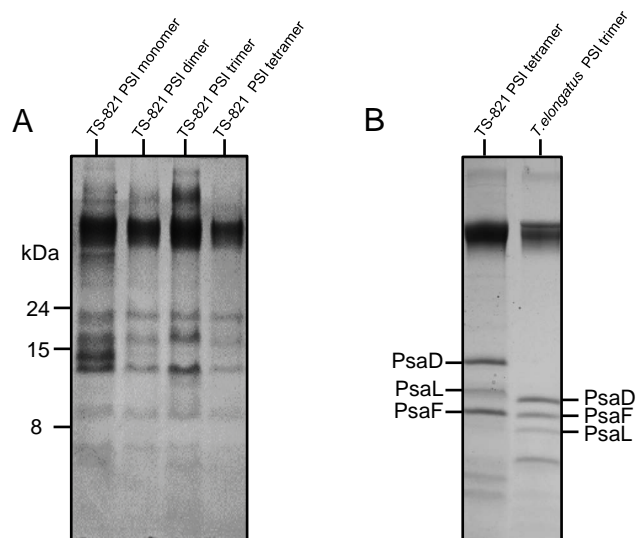
- Almog, O., Shoham, G., Michaeli, D., and Nechushtai, R. (1991). Monomeric and trimeric forms of photosystem I reaction center of *Mastigocladus laminosus*: Crystallization and preliminary characterization. *Proc. Natl. Acad. Sci. USA* **88**: 5312–5316.
- Amunts, A., and Nelson, N. (2008). Functional organization of a plant Photosystem I: Evolution of a highly efficient photochemical machine. *Plant Physiol. Biochem.* **46**: 228–237.
- Amunts, A., and Nelson, N. (2009). Plant photosystem I design in the light of evolution. *Structure* **17**: 637–650.
- Amunts, A., Toporik, H., Borovikova, A., and Nelson, N. (2010). Structure determination and improved model of plant photosystem I. *J. Biol. Chem.* **285**: 3478–3486.
- Aspinwall, C.L., Sarcina, M., and Mullineaux, C.W. (2004). Phycobilisome mobility in the cyanobacterium *Synechococcus* sp. PCC7942 is influenced by the trimerisation of Photosystem I. *Photosynth. Res.* **79**: 179–187.
- Baker, D.R., Manocchi, A.K., Lamicq, M.L., Li, M., Nguyen, K., Sumner, J.J., Bruce, B.D., and Lundgren, C.A. (2014). Comparative photoactivity and stability of isolated cyanobacterial monomeric and trimeric photosystem I. *J. Physiol. Chem. B.* **118**: 2703–2711.
- Ben-Shem, A., Frolow, F., and Nelson, N. (2003). Crystal structure of plant photosystem I. *Nature* **426**: 630–635.
- Ben-Shem, A., Frolow, F., and Nelson, N. (2004). Evolution of photosystem I - from symmetry through pseudo-symmetry to asymmetry. *FEBS Lett.* **564**: 274–280.
- Bibby, T.S., Nield, J., and Barber, J. (2001). Iron deficiency induces the formation of an antenna ring around trimeric photosystem I in cyanobacteria. *Nature* **412**: 743–745.
- Bibby, T.S., Mary, I., Nield, J., Partensky, F., and Barber, J. (2003). Low-light-adapted *Prochlorococcus* species possess specific antennae for each photosystem. *Nature* **424**: 1051–1054.
- Billi, D., Grilli Caiola, M., Paolozzi, L., and Ghelardini, P. (1998). A method for DNA extraction from the desert cyanobacterium *Chroococcidiopsis* and its application to identification of *ftsZ*. *Appl. Environ. Microbiol.* **64**: 4053–4056.
- Boekema, E.J., Dekker, J.P., Vanheel, M.G., Rogner, M., Saenger, W., Witt, I., and Witt, H.T. (1987). Evidence for a trimeric organization of the photosystem I complex from the thermophilic cyanobacterium *Synechococcus* sp. *FEBS Lett.* **217**: 283–286.
- Boekema, E.J., Hifney, A., Yakushevska, A.E., Piotrowski, M., Keegstra, W., Berry, S., Michel, K.P., Pistorius, E.K., and Kruij,

- J. (2001). A giant chlorophyll-protein complex induced by iron deficiency in cyanobacteria. *Nature* **412**: 745–748.
- Boekema, E.J., Van Roon, H., Van Breemen, J.F., and Dekker, J.P. (1999). Supramolecular organization of photosystem II and its light-harvesting antenna in partially solubilized photosystem II membranes. *Eur. J. Biochem.* **266**: 444–452.
- Brecht, M., Hussels, M., Schlodder, E., and Karapetyan, N.V. (2012). Red antenna states of Photosystem I trimers from *Arthrospira platensis* revealed by single-molecule spectroscopy. *Biochim. Biophys. Acta* **1817**: 445–452.
- Cardona, T., Battchikova, N., Zhang, P.P., Stensjö, K., Aro, E.M., Lindblad, P., and Magnuson, A. (2009). Electron transfer protein complexes in the thylakoid membranes of heterocysts from the cyanobacterium *Nostoc punctiforme*. *Biochim. Biophys. Acta* **1787**: 252–263.
- Chitnis, V.P., Xu, Q., Yu, L., Golbeck, J.H., Nakamoto, H., Xie, D.L., and Chitnis, P.R. (1993). Targeted inactivation of the gene *psaL* encoding a subunit of photosystem I of the cyanobacterium *Synechocystis* sp. PCC 6803. *J. Biol. Chem.* **268**: 11678–11684.
- Crisuolo, A., and Gribaldo, S. (2011). Large-scale phylogenomic analyses indicate a deep origin of primary plastids within cyanobacteria. *Mol. Biol. Evol.* **28**: 3019–3032.
- Deusch, O., Landan, G., Roettger, M., Gruenheit, N., Kowallik, K.V., Allen, J.F., Martin, W., and Dagan, T. (2008). Genes of cyanobacterial origin in plant nuclear genomes point to a heterocyst-forming plastid ancestor. *Mol. Biol. Evol.* **25**: 748–761.
- El-Mohsawwy, E., Kopczak, M.J., Schlodder, E., Nowaczyk, M., Meyer, H.E., Warscheid, B., Karapetyan, N.V., and Rögner, M. (2010). Structure and function of intact photosystem 1 monomers from the cyanobacterium *Thermosynechococcus elongatus*. *Biochemistry* **49**: 4740–4751.
- Falcón, L.I., Magallón, S., and Castillo, A. (2010). Dating the cyanobacterial ancestor of the chloroplast. *ISME J.* **4**: 777–783.
- Fewer, D., Friedl, T., and Büdel, B. (2002). Chroococcidiopsis and heterocyst-differentiating cyanobacteria are each other's closest living relatives. *Mol. Phylogenet. Evol.* **23**: 82–90.
- Garczarek, L., van der Staay, G.W.M., Thomas, J.C., and Partensky, F. (1998). Isolation and characterization of Photosystem I from two strains of the marine oxychlorobacterium *Prochlorococcus*. *Photosynth. Res.* **56**: 131–141.
- Gardian, Z., Bumba, L., Schrofel, A., Herbstova, M., Nebesarova, J., and Vacha, F. (2007). Organisation of Photosystem I and Photosystem II in red alga *Cyanidium caldarium*: Encounter of cyanobacterial and higher plant concepts. *Biochim. Biophys. Acta* **1767**: 725–731.
- Gobets, B., van Stokkum, I.H.M., Rögner, M., Kruip, J., Schlodder, E., Karapetyan, N.V., Dekker, J.P., and van Grondelle, R. (2001). Time-resolved fluorescence emission measurements of photosystem I particles of various cyanobacteria: a unified compartmental model. *Biophys. J.* **81**: 407–424.
- Gupta, R.S. (2009). Protein signatures (molecular synapomorphies) that are distinctive characteristics of the major cyanobacterial clades. *Int. J. Syst. Evol. Microbiol.* **59**: 2510–2526.
- Hackenberg, C., Kern, R., Hüge, J., Stal, L.J., Tsuji, Y., Kopka, J., Shiraiwa, Y., Bauwe, H., and Hagemann, M. (2011). Cyanobacterial lactate oxidases serve as essential partners in N_2 fixation and evolved into photorespiratory glycolate oxidases in plants. *Plant Cell* **23**: 2978–2990.
- Hayashi, N.R., Peerapornpisal, Y., Nishihara, H., Ishii, M., Igarashi, Y., and Kodama, T. (1994). Isolation and cultivation of thermophilic cyanobacteria from hot springs of northern thailand. *J. Ferment. Bioeng.* **78**: 179–181.
- Heinemeyer, J., Eubel, H., Wehmhöner, D., Jansch, L., and Braun, H.-P. (2004). Proteomic approach to characterize the supramolecular organization of photosystems in higher plants. *Phytochemistry* **65**: 1683–1692.
- Ihalainen, J.A., D'Haene, S., Yeremenko, N., van Roon, H., Arteni, A.A., Boekema, E.J., van Grondelle, R., Matthijs, H.C.P., and Dekker, J.P. (2005). Aggregates of the chlorophyll-binding protein IsiA (CP43') dissipate energy in cyanobacteria. *Biochemistry* **44**: 10846–10853.
- Ishida, T., Hasegawa, N., Hayashi, N.R., Peerapornpisal, Y., Ishii, M., Igarashi, Y., and Kodama, T. (1997). Growth characteristics and dense culture of a thermophilic cyanobacterium, *Chroococcidiopsis* sp. strain TS-821. *J. Ferment. Bioeng.* **83**: 571–576.
- Ivanov, A.G., Krol, M., Sveshnikov, D., Selstam, E., Sandström, S., Koochek, M., Park, Y.I., Vasil'ev, S., Bruce, D., Oquist, G., and Huner, N.P.A. (2006). Iron deficiency in cyanobacteria causes monomerization of photosystem I trimers and reduces the capacity for state transitions and the effective absorption cross section of photosystem I in vivo. *Plant Physiol.* **141**: 1436–1445.
- Iwamura, T., Nagai, H., and Ichimura, S.-E. (1970). Improved methods for determining contents of chlorophyll, protein, ribonucleic acid, and deoxyribonucleic acid in planktonic populations. *Int. Revue ges. Hydrobiol. Hydrogr.* **55**: 131–147.
- Iwuchukwu, I.J., Vaughn, M., Myers, N., O'Neill, H., Frymier, P., and Bruce, B.D. (2010). Self-organized photosynthetic nanoparticle for cell-free hydrogen production. *Nat. Nanotechnol.* **5**: 73–79.
- Jordan, P., Fromme, P., Witt, H.T., Klukas, O., Saenger, W., and Krauss, N. (2001). Three-dimensional structure of cyanobacterial photosystem I at 2.5 Å resolution. *Nature* **411**: 909–917.
- Karapetyan, N.V., Dorra, D., Schweitzer, G., Bezsmertnaya, I.N., and Holzwarth, A.R. (1997). Fluorescence spectroscopy of the longwave chlorophylls in trimeric and monomeric photosystem I core complexes from the cyanobacterium *Spirulina platensis*. *Biochemistry* **36**: 13830–13837.
- Keeling, P.J. (2004). Diversity and evolutionary history of plastids and their hosts. *Am. J. Bot.* **91**: 1481–1493.
- Kern, R., Bauwe, H., and Hagemann, M. (2011). Evolution of enzymes involved in the photorespiratory 2-phosphoglycolate cycle from cyanobacteria via algae toward plants. *Photosynth. Res.* **109**: 103–114.
- Kiley, P., Zhao, X., Vaughn, M., Baldo, M.A., Bruce, B.D., and Zhang, S. (2005). Self-assembling peptide detergents stabilize isolated photosystem I on a dry surface for an extended time. *PLoS Biol.* **3**: e230.
- Kitmitto, A., Mustafa, A.O., Holzenburg, A., and Ford, R.C. (1998). Three-dimensional structure of higher plant photosystem I determined by electron crystallography. *J. Biol. Chem.* **273**: 29592–29599.
- Kouril, R., Arteni, A.A., Lax, J., Yeremenko, N., D'Haene, S., Rögner, M., Matthijs, H.C.P., Dekker, J.P., and Boekema, E.J. (2005b). Structure and functional role of supercomplexes of IsiA and Photosystem I in cyanobacterial photosynthesis. *FEBS Lett.* **579**: 3253–3257.
- Kouril, R., van Oosterwijk, N., Yakushevskaya, A.E., and Boekema, E.J. (2005). Photosystem I: A search for green plant trimers. *Photochem. Photobiol. Sci.* **4**: 1091–1094.
- Kouril, R., Wientjes, E., Bultema, J.B., Croce, R., and Boekema, E.J. (2013). High-light vs. low-light: Effect of light acclimation on photosystem II composition and organization in *Arabidopsis thaliana*. *Biochim. Biophys. Acta* **1827**: 411–419.
- Kouril, R., Yeremenko, N., D'Haene, S., Oostergetel, G.T., Matthijs, H.C.P., Dekker, J.P., and Boekema, E.J. (2005a). Supercomplexes of IsiA and Photosystem I in a mutant lacking subunit Psal. *Biochim. Biophys. Acta* **1706**: 262–266.
- Kouril, R., Yeremenko, N., D'Haene, S., Yakushevskaya, A.E., Keegstra, W., Matthijs, H.C.P., Dekker, J.P., and Boekema, E.J. (2003). Photosystem I trimers from *Synechocystis* PCC 6803

- lacking the PsaF and PsaJ subunits bind an IsiA ring of 17 units. *Biochim. Biophys. Acta* **1607**: 1–4.
- Kruip, J., Bald, D., Boekema, E., and Rögner, M.** (1994). Evidence for the existence of trimeric and monomeric Photosystem I complexes in thylakoid membranes from cyanobacteria. *Photosynth. Res.* **40**: 279–286.
- Kruip, J., Boekema, E.J., Bald, D., Boonstra, A.F., and Rögner, M.** (1993). Isolation and structural characterization of monomeric and trimeric photosystem I complexes (P700.F_A/F_B and P700.F_X) from the cyanobacterium *Synechocystis* PCC 6803. *J. Biol. Chem.* **268**: 23353–23360.
- Kruip, J., Chitnis, P.R., Lagoutte, B., Rögner, M., and Boekema, E.J.** (1997). Structural organization of the major subunits in cyanobacterial photosystem I. Localization of subunits PsaC, -D, -E, -F, and -J. *J. Biol. Chem.* **272**: 17061–17069.
- LeBlanc, G., Chen, G., Jennings, G.K., and Cliffler, D.E.** (2012). Photoreduction of catalytic platinum particles using immobilized multilayers of Photosystem I. *Langmuir* **28**: 7952–7956.
- Mangels, D., Kruip, J., Berry, S., Rögner, M., Boekema, E.J., and Koenig, F.** (2002). Photosystem I from the unusual cyanobacterium *Gloeobacter violaceus*. *Photosynth. Res.* **72**: 307–319.
- Mareš, J., Hrouzek, P., Kaňa, R., Ventura, S., Strunecký, O., and Komárek, J.** (2013). The primitive thylakoid-less cyanobacterium *gloeobacter* is a common rock-dwelling organism. *PLoS ONE* **8**: e66323.
- Mershin, A., Matsumoto, K., Kaiser, L., Yu, D., Vaughn, M., Nazeeruddin, M.K., Bruce, B.D., Graetzel, M., and Zhang, S.** (2012). Self-assembled photosystem-I biophotovoltaics on nanostructured TiO₂ and ZnO. *Sci Rep* **2**: 234.
- Mukherjee, D., Vaughn, M., Khomami, B., and Bruce, B.D.** (2011). Modulation of cyanobacterial photosystem I deposition properties on alkanethiolate Au substrate by various experimental conditions. *Colloids Surf. B Biointerfaces* **88**: 181–190.
- Nelson, N., and Ben-Shem, A.** (2005). The structure of photosystem I and evolution of photosynthesis. *Bioessays* **27**: 914–922.
- Nelson, N., and Yocum, C.F.** (2006). Structure and function of photosystems I and II. *Annu. Rev. Plant Biol.* **57**: 521–565.
- Nesterenko, M.V., Tilley, M., and Upton, S.J.** (1994). A simple modification of Blum's silver stain method allows for 30 minute detection of proteins in polyacrylamide gels. *J. Biochem. Biophys. Methods* **28**: 239–242.
- Notredame, C., Higgins, D.G., and Heringa, J.** (2000). T-Coffee: A novel method for fast and accurate multiple sequence alignment. *J. Mol. Biol.* **302**: 205–217.
- Olson, D.G., Tripathi, S.A., Giannone, R.J., Lo, J., Caiazza, N.C., Hogsett, D.A., Hettich, R.L., Guss, A.M., Dubrovsky, G., and Lynd, L.R.** (2010). Deletion of the Cel48S cellulase from *Clostridium thermocellum*. *Proc. Natl. Acad. Sci. USA* **107**: 17727–17732.
- Onai, K., Morishita, M., Kaneko, T., Tabata, S., and Ishiura, M.** (2004). Natural transformation of the thermophilic cyanobacterium *Thermosynechococcus elongatus* BP-1: A simple and efficient method for gene transfer. *Mol. Genet. Genomics* **271**: 50–59.
- Oostergetel, G.T., Keegstra, W., and Brisson, A.** (1998). Automation of specimen selection and data acquisition for protein electron crystallography. *Ultramicroscopy* **74**: 47–59.
- Schägger, H.** (2006). Tricine-SDS-PAGE. *Nat. Protoc.* **1**: 16–22.
- Schägger, H., and von Jagow, G.** (1991). Blue native electrophoresis for isolation of membrane protein complexes in enzymatically active form. *Anal. Biochem.* **199**: 223–231.
- Schlodder, E., Hussels, M., Cetin, M., Karapetyan, N.V., and Brecht, M.** (2011). Fluorescence of the various red antenna states in photosystem I complexes from cyanobacteria is affected differently by the redox state of P700. *Biochim. Biophys. Acta* **1807**: 1423–1431.
- Schluchter, W.M., Shen, G.H., Zhao, J.D., and Bryant, D.A.** (1996). Characterization of *psaI* and *psaL* mutants of *Synechococcus* sp. strain PCC 7002: A new model for state transitions in cyanobacteria. *Photochem. Photobiol.* **64**: 53–66.
- Shih, P.M., et al.** (2013). Improving the coverage of the cyanobacterial phylum using diversity-driven genome sequencing. *Proc. Natl. Acad. Sci. USA* **110**: 1053–1058.
- Tabb, D.L., Fernando, C.G., and Chambers, M.C.** (2007). MyriMatch: Highly accurate tandem mass spectral peptide identification by multivariate hypergeometric analysis. *J. Proteome Res.* **6**: 654–661.
- Tamura, K., Peterson, D., Peterson, N., Stecher, G., Nei, M., and Kumar, S.** (2011). MEGA5: Molecular evolutionary genetics analysis using maximum likelihood, evolutionary distance, and maximum parsimony methods. *Mol. Biol. Evol.* **28**: 2731–2739.
- Tsotis, G., Haase, W., Engel, A., and Michel, H.** (1995). Isolation and structural characterization of trimeric cyanobacterial photosystem I complex with the help of recombinant antibody fragments. *Eur. J. Biochem.* **231**: 823–830.
- Tucker, D.L., and Sherman, L.A.** (2000). Analysis of chlorophyll-protein complexes from the cyanobacterium *Cyanothece* sp. ATCC 51142 by non-denaturing gel electrophoresis. *Biochim. Biophys. Acta* **1468**: 150–160.
- Umena, Y., Kawakami, K., Shen, J.-R., and Kamiya, N.** (2011). Crystal structure of oxygen-evolving photosystem II at a resolution of 1.9 Å. *Nature* **473**: 55–60.
- Veith, T., and Büchel, C.** (2007). The monomeric photosystem I-complex of the diatom *Phaeodactylum tricornutum* binds specific fucoxanthin chlorophyll proteins (FCPs) as light-harvesting complexes. *Biochim. Biophys. Acta* **1767**: 1428–1435.
- Washburn, M.P., Wolters, D., and Yates, J.R., III.** (2001). Large-scale analysis of the yeast proteome by multidimensional protein identification technology. *Nat. Biotechnol.* **19**: 242–247.
- Watanabe, M., Iwai, M., Narikawa, R., and Ikeuchi, M.** (2009). Is the photosystem II complex a monomer or a dimer? *Plant Cell Physiol.* **50**: 1674–1680.
- Watanabe, M., Kubota, H., Wada, H., Narikawa, R., and Ikeuchi, M.** (2011). Novel supercomplex organization of photosystem I in *Anabaena* and *Cyanophora paradoxa*. *Plant Cell Physiol.* **52**: 162–168.
- Watanabe, M., Semchonok, D.A., Webber-Birungi, M.T., Ehira, S., Kondo, K., Narikawa, R., Ohmori, M., Boekema, E.J., and Ikeuchi, M.** (2014). Attachment of phycobilisomes in an antenna-photosystem I supercomplex of cyanobacteria. *Proc. Natl. Acad. Sci. USA* **111**: 2512–2517.
- Waterbury, J.B., and Stanier, R.Y.** (1978). Patterns of growth and development in pleurocapsalean cyanobacteria. *Microbiol. Rev.* **42**: 2–44.
- Wittig, I., Braun, H.-P., and Schägger, H.** (2006). Blue native PAGE. *Nat. Protoc.* **1**: 418–428.
- Xu, Q., Hoppe, D., Chitnis, V.P., Odom, W.R., Guikema, J.A., and Chitnis, P.R.** (1995). Mutational analysis of photosystem I polypeptides in the cyanobacterium *Synechocystis* sp. PCC 6803. Targeted inactivation of *psaI* reveals the function of *psaI* in the structural organization of *psaL*. *J. Biol. Chem.* **270**: 16243–16250.
- Xu, W., Tang, H.D., Wang, Y.C., and Chitnis, P.R.** (2001). Proteins of the cyanobacterial photosystem I. *Biochim. Biophys. Acta* **1507**: 32–40.
- Zang, X., Liu, B., Liu, S., Arunakumara, K.K., and Zhang, X.** (2007). Optimum conditions for transformation of *Synechocystis* sp. PCC 6803. *J. Microbiol.* **45**: 241–245.



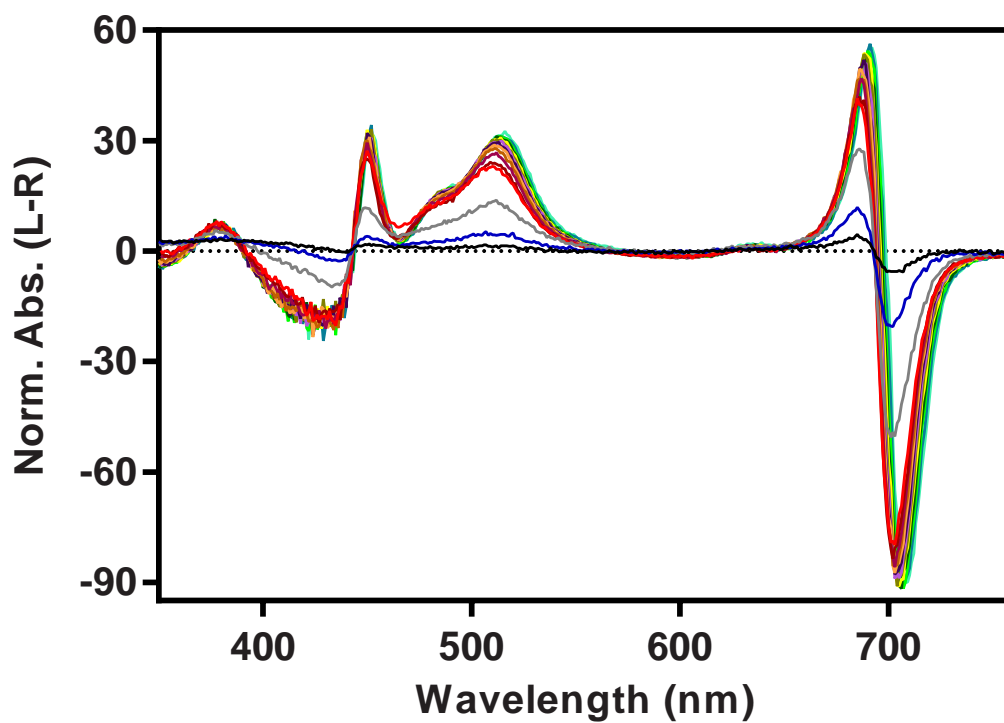
Supplemental Figure 1. Molecular weight Estimation of TS-821 PSI Using BN-PAGE. Protein MW standards (Invitrogen) were initially used for molecular weights estimation. According to the fit (dash line) and the reported known photosystem crystal structures, the calculated molecular weights for *T. elongatus* PSI trimer and PSII dimer were underestimated. To estimate the molecular weights of TS-821 PSI, the photosystems from *T. elongatus* were used as molecular weight standards. The R^2 values of linear fits using protein MW standards (dash line) and *T. elongatus* photosystems (solid line) are 0.985 and 0.999 respectively. The calculated molecular weights for the three major green bands (Figure 1A) are 400 kDa, 800 kDa, and 1600 kDa which represents the PSI monomer (M), dimer (D), and tetramer (T) respectively.



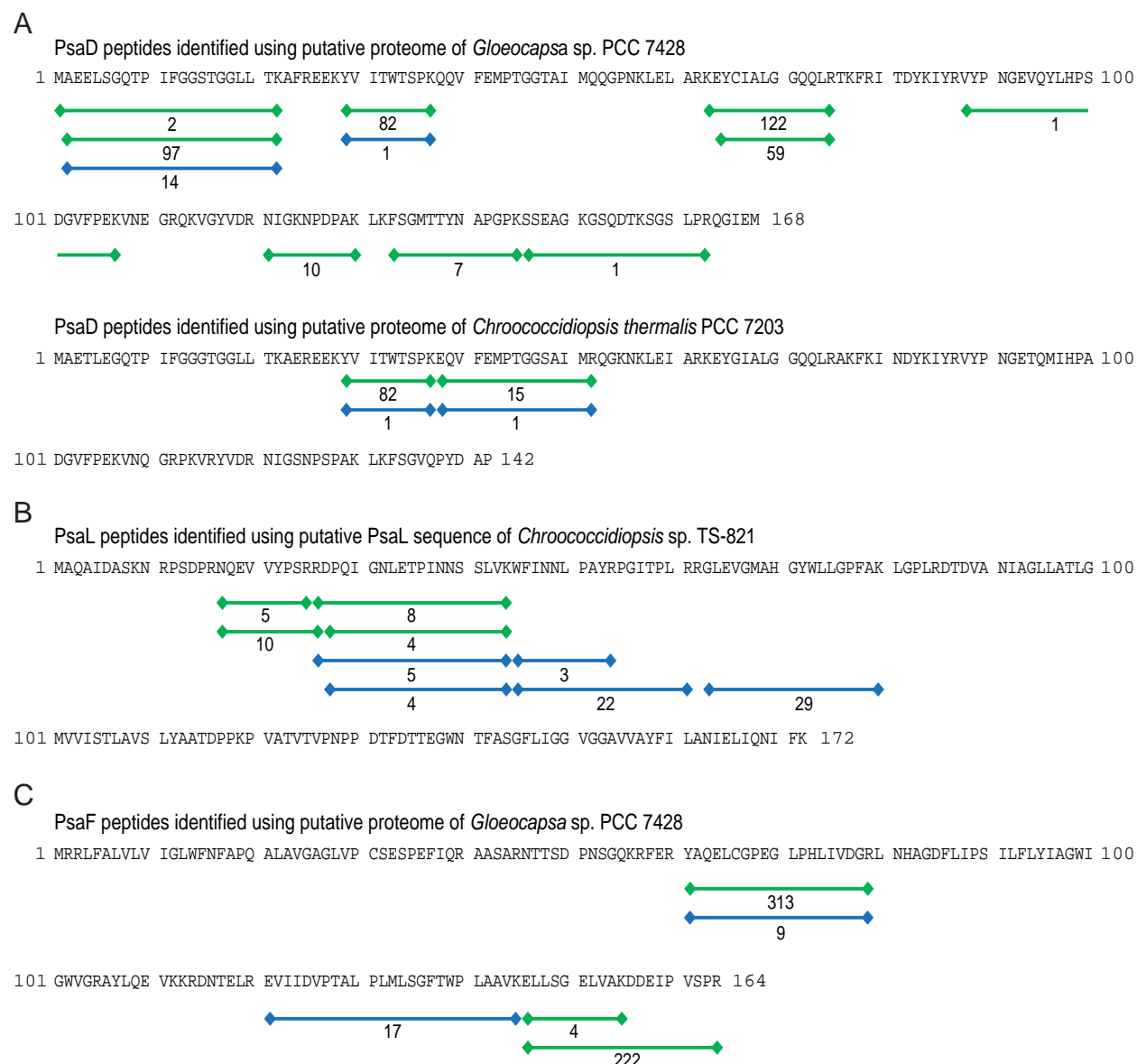
Supplemental Figure 2. SDS-PAGE of TS-821 PSI and *T. elongatus* PSI.

(A) SDS-PAGE of isolated TS-821 PSI monomer, dimer, trimer, and tetramer from second SDGC (Figure 2B).

(B) SDS-PAGE of isolated TS-821 PSI tetramer and *T. elongatus* PSI trimer. The PsaD, PsaF and PsaL subunits are labeled.



Supplemental Figure 3. CD spectra of TS-821 PSI tetramer at different temperatures. As temperature goes up from 15°C to 90°C by 5°C steps, the peak values decrease.



Supplemental Figure 4. LC-MS/MS Identification of Subunits in TS-821 PSI Tetramer.

(A) TS-821 PsaD peptides identified by searching against proteomes of *Gloeocapsa* sp. PCC 7428 and *Chroococcidiopsis thermalis* PCC 7203.

(B) TS-821 PsaL peptides identified by searching against TS-821 PsaL sequence.

(C) TS-821 PsaF peptides identified by searching against proteome of *Gloeocapsa* sp. PCC 7428.

Distinct peptides identified using PSI tetramer whole protein complex and separated bands after SDS-PAGE (Supplemental Figure 2B) are denoted using green and blue bars respectively. The number of filtered spectra for each distinct peptide is shown under the bar.

Supplemental Figure 5. PsaL Alignment for Phylogenetic Analysis.

Strains that have two different PsaL sequences are highlighted in accordance with Figure 8B. The following major clades are denoted to the left of the strain names: Viridiplantae (V), Rhodoplantae (R), and cyanobacterial clades (I, II, and III).

V	<i>Arabidopsis thaliana</i>	QVVQPIINGDPFPGISLETPVTSSPLIAWYLSNLPGYRTAVNPLLRGVEVGLAHGFFLVGPFPVKAGPLRNT-AYAGSAGSLAAAGLVVILSM
	<i>Oryza sativa</i> subsp japonica	QVVQPIINGDPFPGISLETPVTSSPLVAVYLSNLPAYRTAVSPLLRGIEVGLAHGYLLVGPFPALTGPLRNT-PVHQAGALGAAGLVAILSV
	<i>Ostreococcus lucimarinus</i> CCE9901	QI IKP IINGDPFPGISLETPVTSSPDVANFVLSNLPAYRTGVAPVLRGVEVGLAHGFFLTGPFKIKGLPLRST-DAEELAGCLSGAGLVILTA
	<i>Chlamydomonas reinhardtii</i>	QVISPVNGDPFVGMLETPVTSAPIVATYLSNLPAYRTGVAPVLRGVEIGLAHGFLLAGPFIKGLPLRNPETAIEIAGSLSAAGLVILAL
	<i>Porphyra purpurea</i>	EFIKPYNDPDPFVGNLSTPVSTSSFSKGLLGNLPAYRRLGSPLLRGLIEIGMAHGYPFLIGPFDKGLPLRGT-DVALLAGFLSSVGLIILITTT
R	<i>Cyanidioschyzon merolae</i>	DYIKPYNDPDPFVGHLPATPINSSSLTRAYLSQLPIYRRGVSPFLRGLIEIGMAHGYPFLIGPFPVQLGPLRNT-PADKYLAGLSSAIGLIVITLT
	<i>Cyanidium caldarium</i>	NYIKPYGNSNPFVGNLSTPVNSKVTIWIYLNKLPYIRRGVSPLLRGLIEIGMAHGYPFLIGPFPYKGLPLRNT-DLSLLSGLIAAIGLIIIISSI
	<i>Thermosynechococcus elongatus</i> BP-1	ELVKPYNGDPFVGHLPSTPISDSGLVKTPIGNLPAYRQGLSPILRGLIEVGMAGHYFLIGPWWKGLPLRDS-DVANLGGILSGIALILVATA
	<i>Arthrospira platensis</i> NIES-39	GLIQAYNGDPFVGHLPSTPISDSAPTRTFIGNLPAYRPGLSPLLRGLIEIGMAHGYPFLIGPWWKFGTQRGT-EFANLNGLICGLAMLLIATA
	<i>Trichodesmium erythraeum</i> IMS101	GFVQPYKGDPPFVGHLPSTPISDSDFTRAFIGNLPYRPGLSPLLRGLIEVGMAGHYFIVGPWTKGLPLRDS-AVANLGGILSTIALVLIATI
I	<i>Chroococcidiopsis</i> sp. PCC 6712	QVVKPYNDPDPFVGHLPSTPISASDFTKTFIGNLPAYRKGVLAPILRGLIEVGMAGHYFLVGPWWVGLPLRDS-EFASLGGILSALAMVLIATA
	<i>Microcystis aeruginosa</i> NIES-843	QVVTPYNDPDPFVGHLPSTPISASDFTKTFIGNLPAYRPGLSPLLRGLIEIGMAHGYPFLIGPWWVGLPLRDS-EFANLGGILPALAMVLIATA
	<i>Pleurocapsa</i> sp. PCC 7327	QVVQPYNGDPFVGHLPSTPISASDFTKTFIGNLPAYRPGLSPLLRGLIEIGMAHGYPFLIGPWWVGLPLRDS-EFASLGGILSGLAILIATA
	<i>Synechocystis</i> PCC 6803	QVVQAYNGDPFVGHLPSTPISDSAPTRTFIGNLPAYRKGSLPILRGLIEVGMAGHYFLIGPWWVGLPLRDS-EYQYIGGLIGALAILVATA
	<i>Synechococcus</i> sp. JA-2-3B'a(2-13)	DYIRTFNDPDPFVGHLPSTPISDSPVTRTFIGNLPAYRPGLSPLLRGLIEIGMAHGYPFLIGPWWVGLPLRDS-EFASLGGILSGLAILIATA
II	<i>Oscillatoria</i> sp. PCC 7112	ELIKPFNGDPFVGHLPSTPISASDFTKTFIGNLPAYRKGSLPILRGLIEIGMAHGYPFLIGPWWVGLPLRDS-EYQYIGGLIGALAILVATA
	<i>Microcoleus chthonoplastes</i> PCC 7420	EMVKPYGDPFVGHLPSTPISDSAPTRAFIGNLPAYRKGSLPILRGLIEIGMAHGYPFLIGPWWVGLPLRDS-EYQYIGGLIGALAILVATA
	<i>Cyanotheca</i> sp. ATCC 51142	QMVKAYKDDPFVGHLPSTPISDSGTFRAFIGNLPAYRKGSLPILRGLIEIGMAHGYPFLIGPWWVGLPLRDS-EYQYIGGLIGALAILVATA
	<i>Calothrix</i> sp. PCC 7507	DI IKPFKGDPCGLNLSTPINDSPLVRAFISNLPAYRKGSLPILRGLIEIGMAHGYPFLIGPWWVGLPLRDS-EYQYIGGLIGALAILVATA
	<i>Fischerella</i> sp. JSC-11	DI IKPFKGDPCGLNLSTPINDSPLAKAFINNLPAYRKGSLPILRGLIEIGMAHGYPFLIGPWWVGLPLRDS-EYQYIGGLIGALAILVATA
III	<i>Fischerella</i> sp. PCC 9605	DI IKPFKGDPCGLNLSTPINDSPLARAFINNLPAYRKGSLPILRGLIEIGMAHGYPFLIGPWWVGLPLRDS-EYQYIGGLIGALAILVATA
	<i>Chroococcidiopsis thermalis</i> PCC 7203	DPVQPYKGDPPFNSFTAITDSPLARAFINNLPAYRKGSLPILRGLIEIGMAHGYPFLIGPWWVGLPLRDS-EYQYIGGLIGALAILVATA
	<i>Synechococcus</i> sp. PCC 7335	DPVQPYKGDPPFNSFTAITDSPLARAFINNLPAYRKGSLPILRGLIEIGMAHGYPFLIGPWWVGLPLRDS-EYQYIGGLIGALAILVATA
	<i>Pleurocapsa</i> sp. PCC 7327	DPVQPYKGDPPFNSFTAITDSPLARAFINNLPAYRKGSLPILRGLIEIGMAHGYPFLIGPWWVGLPLRDS-EYQYIGGLIGALAILVATA
	<i>Synechococcus</i> sp. PCC 7335	DPVQPYKGDPPFNSFTAITDSPLARAFINNLPAYRKGSLPILRGLIEIGMAHGYPFLIGPWWVGLPLRDS-EYQYIGGLIGALAILVATA
III	<i>Gloeocapsa</i> sp. PCC 73106	DPVQPYKGDPPFNSFTAITDSPLARAFINNLPAYRKGSLPILRGLIEIGMAHGYPFLIGPWWVGLPLRDS-EYQYIGGLIGALAILVATA
	<i>Synechococcus</i> sp. PCC 7002	DPVQPYKGDPPFNSFTAITDSPLARAFINNLPAYRKGSLPILRGLIEIGMAHGYPFLIGPWWVGLPLRDS-EYQYIGGLIGALAILVATA
	<i>Prochlorococcus marinus</i> MIT 9313	DPVQPYKGDPPFNSFTAITDSPLARAFINNLPAYRKGSLPILRGLIEIGMAHGYPFLIGPWWVGLPLRDS-EYQYIGGLIGALAILVATA
	<i>Prochlorococcus marinus</i> SS120	DPVQPYKGDPPFNSFTAITDSPLARAFINNLPAYRKGSLPILRGLIEIGMAHGYPFLIGPWWVGLPLRDS-EYQYIGGLIGALAILVATA
	<i>Synechococcus elongatus</i> PCC 7942	DPVQPYKGDPPFNSFTAITDSPLARAFINNLPAYRKGSLPILRGLIEIGMAHGYPFLIGPWWVGLPLRDS-EYQYIGGLIGALAILVATA
III	<i>Crocospheara watsonii</i> WH 8501	DPVQPYKGDPPFNSFTAITDSPLARAFINNLPAYRKGSLPILRGLIEIGMAHGYPFLIGPWWVGLPLRDS-EYQYIGGLIGALAILVATA
	<i>Cyanotheca</i> sp. ATCC 51142	DPVQPYKGDPPFNSFTAITDSPLARAFINNLPAYRKGSLPILRGLIEIGMAHGYPFLIGPWWVGLPLRDS-EYQYIGGLIGALAILVATA
	<i>Pleurocapsa</i> sp. PCC 7319	DPVQPYKGDPPFNSFTAITDSPLARAFINNLPAYRKGSLPILRGLIEIGMAHGYPFLIGPWWVGLPLRDS-EYQYIGGLIGALAILVATA
	<i>Xenococcus</i> sp. PCC 7305	DPVQPYKGDPPFNSFTAITDSPLARAFINNLPAYRKGSLPILRGLIEIGMAHGYPFLIGPWWVGLPLRDS-EYQYIGGLIGALAILVATA
	<i>Gloeocapsa</i> sp. PCC 7428	DPVQPYKGDPPFNSFTAITDSPLARAFINNLPAYRKGSLPILRGLIEIGMAHGYPFLIGPWWVGLPLRDS-EYQYIGGLIGALAILVATA
III	<i>Chroococcidiopsis</i> sp. TS-821	DPVQPYKGDPPFNSFTAITDSPLARAFINNLPAYRKGSLPILRGLIEIGMAHGYPFLIGPWWVGLPLRDS-EYQYIGGLIGALAILVATA
	<i>Chroococcidiopsis thermalis</i> PCC 7203	DPVQPYKGDPPFNSFTAITDSPLARAFINNLPAYRKGSLPILRGLIEIGMAHGYPFLIGPWWVGLPLRDS-EYQYIGGLIGALAILVATA
	<i>Fischerella</i> sp. JSC-11	DPVQPYKGDPPFNSFTAITDSPLARAFINNLPAYRKGSLPILRGLIEIGMAHGYPFLIGPWWVGLPLRDS-EYQYIGGLIGALAILVATA
	<i>Fischerella</i> sp. PCC 9605	DPVQPYKGDPPFNSFTAITDSPLARAFINNLPAYRKGSLPILRGLIEIGMAHGYPFLIGPWWVGLPLRDS-EYQYIGGLIGALAILVATA
	<i>Mastigocladopsis repens</i> PCC 10914	DPVQPYKGDPPFNSFTAITDSPLARAFINNLPAYRKGSLPILRGLIEIGMAHGYPFLIGPWWVGLPLRDS-EYQYIGGLIGALAILVATA
III	<i>Mastigocladus laminosus</i>	DPVQPYKGDPPFNSFTAITDSPLARAFINNLPAYRKGSLPILRGLIEIGMAHGYPFLIGPWWVGLPLRDS-EYQYIGGLIGALAILVATA
	<i>Nostoc punctiforme</i> ATCC 29133	DPVQPYKGDPPFNSFTAITDSPLARAFINNLPAYRKGSLPILRGLIEIGMAHGYPFLIGPWWVGLPLRDS-EYQYIGGLIGALAILVATA
	<i>Anabaena variabilis</i> ATCC 29413	DPVQPYKGDPPFNSFTAITDSPLARAFINNLPAYRKGSLPILRGLIEIGMAHGYPFLIGPWWVGLPLRDS-EYQYIGGLIGALAILVATA
	<i>Nostoc</i> sp. PCC 7120	DPVQPYKGDPPFNSFTAITDSPLARAFINNLPAYRKGSLPILRGLIEIGMAHGYPFLIGPWWVGLPLRDS-EYQYIGGLIGALAILVATA
	<i>Calothrix</i> sp. PCC 7507	DPVQPYKGDPPFNSFTAITDSPLARAFINNLPAYRKGSLPILRGLIEIGMAHGYPFLIGPWWVGLPLRDS-EYQYIGGLIGALAILVATA
III	<i>Nostoc azollae</i> 0708	DPVQPYKGDPPFNSFTAITDSPLARAFINNLPAYRKGSLPILRGLIEIGMAHGYPFLIGPWWVGLPLRDS-EYQYIGGLIGALAILVATA
	<i>Cylindrospermopsis raciborskii</i> CS-505	DPVQPYKGDPPFNSFTAITDSPLARAFINNLPAYRKGSLPILRGLIEIGMAHGYPFLIGPWWVGLPLRDS-EYQYIGGLIGALAILVATA
	<i>Raphidiopsis brookii</i> D9	DPVQPYKGDPPFNSFTAITDSPLARAFINNLPAYRKGSLPILRGLIEIGMAHGYPFLIGPWWVGLPLRDS-EYQYIGGLIGALAILVATA
	<i>Synechococcus</i> sp. JA-2-3B'a(2-13)	DPVQPYKGDPPFNSFTAITDSPLARAFINNLPAYRKGSLPILRGLIEIGMAHGYPFLIGPWWVGLPLRDS-EYQYIGGLIGALAILVATA
	<i>Gloeobacter violaceus</i> PCC 7421	DPVQPYKGDPPFNSFTAITDSPLARAFINNLPAYRKGSLPILRGLIEIGMAHGYPFLIGPWWVGLPLRDS-EYQYIGGLIGALAILVATA

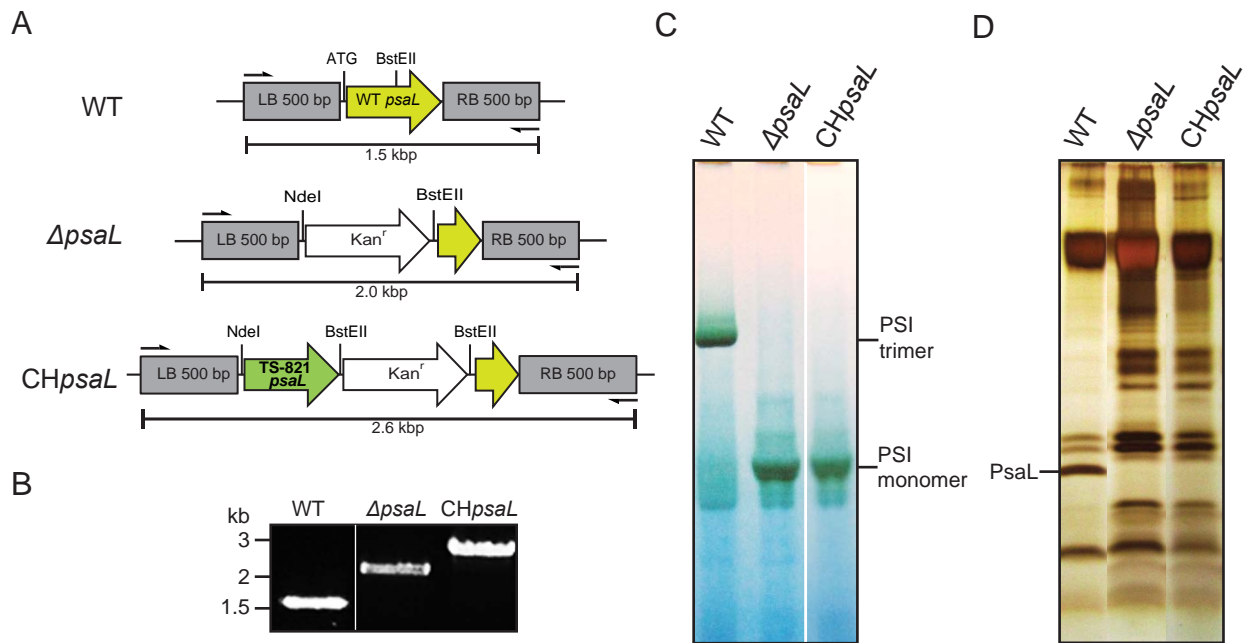
V
R

Arabidopsis thaliana
Oryza sativa subsp *japonica*
Ostreococcus lucimarinus CCE9901
Chlamydomonas reinhardtii
Porphyra purpurea
Cyanidioschyzon merolae
Cyanidium caldarium
Thermosynechococcus elongatus BP-1
Arthrospira platensis NIES-39
Trichodesmium erythraeum IMS101
Chroococcidiopsis sp. PCC 6712
Microcystis aeruginosa NIES-843
Pleurocapsa sp. PCC 7327
Synechocystis PCC 6803
Synechococcus sp. JA-2-3B'a(2-13)
Oscillatoria sp. PCC 7112
Microcoleus chthonoplastes PCC 7420
Cyanotheca sp. ATCC 51142
Calothrix sp. PCC 7507
Fischerella sp. JSC-11
Fischerella sp. PCC 9605
Chroococcidiopsis thermalis PCC 7203
Synechococcus sp. PCC 7335
Pleurocapsa sp. PCC 7327
Synechococcus sp. PCC 7335
Gloeocapsa sp. PCC 73106
Synechococcus sp. PCC 7002
Prochlorococcus marinus MIT 9313
Prochlorococcus marinus SS120
Synechococcus elongatus PCC 7942
Crocospaera watsonii WH 8501
Cyanotheca sp. ATCC 51142
Pleurocapsa sp. PCC 7319
Xenococcus sp. PCC 7305
Gloeocapsa sp. PCC 7428
Chroococcidiopsis sp. TS-821
Chroococcidiopsis thermalis PCC 7203
Fischerella sp. JSC-11
Fischerella sp. PCC 9605
Mastigocladopsis repens PCC 10914
Mastigocladus laminosus
Nostoc punctiforme ATCC 29133
Anabaena variabilis ATCC 29413
Nostoc sp. PCC 7120
Calothrix sp. PCC 7507
Nostoc azollae 0708
Cylindrospermopsis raciborskii CS-505
Raphidiopsis brookii D9
Synechococcus sp. JA-2-3B'a(2-13)
Gloeobacter violaceus PCC 7421

II

III

CLTIYGISSFKEGEPSIAPSLTLTGRRKKQPDQLQTADGWAKFTGGFFFGGIGSVTWAYFLLYV--LDLPYFVK-----
 CLTMYGVASFGEGEPSTAPTTLTLTGRRKKEADKLQTADGWAKFTGGFFFGGIGSVLWAYFLLYV--LDLPYFFK-----
 CLSIYGATAFQREEVVGLKTLSGRAIAKDP--LQSSDGWASFTSGWLVGSLGVAWSYVLTQV--LPYYS-----
 CLSIYGSAQFQSTPSIGVITLSGRSVARDP--LFSADGWSEFAAGFLVGGAGVAVAYVCTQI--LPYYS-----
 CLSMYGNVS-----FTRSDSKDP--LQTAEGWQQTAGFLVGAVGGSGFAYLLLAN--IPVLQTAGLSLFS-----
 GMLLYGAVS-----FTNDSQD--LESVDGWRLQASGFLLGAVGGAGFAYLLTL--FS-----
 AMIYIGVITFPDENSEN-----NDK--LQTANGWRQLASGFLLGAVGGAGFAYILLANNLLSTSTPILQT-----
 CLAAYGLVSFQKGGG-----SSDP--LKTSEGWSQFTAGFFVGMAGSAFVAFLLLEN--FSVVDGIMTGLFN-----
 CLAAYGLVTFQGDKS-----EGDS--LQSAAGWSQFAGGFFIGMGSAFVAFLLLEN--FAVVDAILFRGLVNN-----
 CLSAYGLVSFQKQSP-----EGADP--LKTSEGWSQFTAGGFFIGMGSAFVAFLLLEN--FELVDISIFRGLFNS-----
 CLSIYGIAT-----FQDKPTNSEDG--LQSSSEGWSQFAAGFFIGMGSAFVAFVLLQ--PDVVDNIFRGLVNN-----
 CLASYGLVSFQKGA--IGTGDA--SNDP--LKSSEGWSQFAAGFFIGMGSAFVAFVLLLEN--LGVVDGIMRGLVFNQ-----
 CLASYGLVSFQGGRA--IGTGDA--LKSSEGWSQFTAGFFVGMGGAFVAFVLLLEN--LGVIDAIMRGLVNN-----
 ALSYGLVTFQGEQ--SGDT--LQTADGWQFAAGFFVGMGGAFVAFVLLLEN--LSVVDGIFRGLFN-----
 CMSAYGSVT-FGNKP--ETPGAAP-----LATARGWDLTAGFFLGGMGVFAAYFLLEN--LQDAIFRGLVNN-----
 GMSAYGLVSFKQDNT--SYPSANPMT--DS--LRNAEGWSQFTAGFFIGMGVFAAYFLLEN--LQGVDAIFRGLVNN-----
 GMAANGLVS-----LKSASESAPDTL--LKTSEGWSQFAAGFFVGMGGAFVAFVLLLEN--FETVDAIFRGLVNN-----
 GLNAHGLVS-----LKSASESAPDTA--MQTSEGWSLFASGFFLGSTGSAPFVAFVLLLEN--FSTIDAIFRGLVNN-----
 GISIFAITTFQGNPR--GAYNSYKDLRLP--LKTREWSQLNGGIFIGMGGAIFAYFLLEN--FDSLDAILRGAVNAS-----
 GISIFAITTFQGNPK--GSYSSYKDSLRLP--LRTREWSQLNGGIFIGMGGAIFAYFLLEN--FDALDAILRGAVNAS-----
 GISIFAITTFQGNPK--GSYSSYKDSLRLP--LRTREWSQLNGGIFIGMGGAIFAYFLLEN--FDSLDAILRGAVNVSYLSF-----
 GISIFAITTFQGDPR--GAYGSTSKDSLRLP--LRNRDEWYQLNGGIFIGMGGAIFAYFLLEN--FDALDAILRGAVNVN-----
 GISIFALATFQGDPR--GTYNHSHRDLRLP--LRKKEDWYQLSGGILMGSILGGAIFAYFLLEN--FELDLISILRGAVNVG-----
 GISIFALAMFQNNPK--GSYNSYKDLRLP--LRSKEDWYQLAGGVFLGSMGGAIFAYFLLEN--FDDLDAILRGAVNLPWVTG-----
 CLSIYGGAD--VSSE--ISRNTLPYQPPPEA--LSTDEGWSEFAGSFLIGGIGGAIFAYFLLEN--LPLLLGSIGA-----
 GLSLHGAVR--TEKA--TATLTPPQPPVD--FATTEGWSEFAGSFLIGGIGGAIFAYFLATT--PLLQAFNR-----
 ALSLYGSVG--VSTP--TATLTPPQPPVD--EN--LGTKEGWSEFAGSFLIGGIGGAIFAYFLATT--PLMYYTI-----
 LLVLYNVPGKAPTVP--PPDVTVANPPAD--LFTKRGWADFTSGFWLGGCAGAFVAFVLLLEN--LHMQPILLNVPMNVWAS-----
 LLVLYNAPGKAPNIQ--PSDCTINNPPAD--LFTKRGWADFTSGFWLGGCAGAFVAFVLLLEN--LHMQPILLNVPMNVWAS-----
 CLSLYGNAGSGPSAA--ESTVITPNPPQE--LFTKGEWSEFTSGFWLGGCAGAFVAFVLLLEN--LHMQPILLNVPMNVWAS-----
 ALSMYASVG--VTKP--TETLTPPQPPVD--EA--LATSEGWSEFAGSFLIGGIGGAIFAYFLATT--PLLQAFNR-----
 ALSLYASVE--VGKP--IETLTPPQPPVD--LGTSGWSEFAGSFLIGGIGGAIFAYFLATT--PLLQAFNR-----
 CLSLYASAM--GGKP--SETLTAPKVP--AA--FASKEGWSEFATGFFLGGSGGAIFAYFLATT--PLLQAFNR-----
 ALSLYASAM--GGAP--VSVITAPNTPE--LGTKEGWSEFATGFFLGGSGGAIFAYFLATT--PLLQAFNR-----
 AMSLYAATD--PPKP--VATVTPNPP--DT--FDTTEGWNTYASGFLIGGIGGAIFAYFLATT--PLLQAFNR-----
 AVSLYAATD--PPKP--VATVTPNPP--DT--FDTTEGWNTYASGFLIGGIGGAIFAYFLATT--PLLQAFNR-----
 TMLYASASN--PPQP--VATTTTGGQVST--FKSPESWNNYISGFLIGGIGGAIFAYFLATT--PLLQAFNR-----
 ALSLYASNSN--PPEP--VASVTAPHP--DA--FHTKEGWNTYASGFLIGGIGGAIFAYFLATT--PLLQAFNR-----
 ALSLYASNSN--PPQP--VASVTAPHP--DA--FHTKEGWNTYASGFLIGGIGGAIFAYFLATT--PLLQAFNR-----
 ALSLYASNSN--PPQP--VASVTAPHP--DA--FHTKEGWNTYASGFLIGGIGGAIFAYFLATT--PLLQAFNR-----
 CLSLYASNSN--PPQP--HVTITTPNPP--DA--FRSKEGWNTYASGFLIGGIGGAIFAYFLATT--PLLQAFNR-----
 ALTLYASNSK--PPKP--VKSATPNTPE--EA--FQSSEGWNNTYASGFLIGGIGGAIFAYFLATT--PLLQAFNR-----
 ALSLYASNSN--PPKA--LPSVTVPNPPVDA--FNSKEGWNTYASGFLIGGIGGAIFAYFLATT--PLLQAFNR-----
 SLSLYASNSN--PPKA--LASVTVPNPP--DA--FQSKEGWNTYASGFLIGGIGGAIFAYFLATT--PLLQAFNR-----
 ALSLYASNSN--PPTA--LASVTVPNPP--DA--FQSKEGWNTYASGFLIGGIGGAIFAYFLATT--PLLQAFNR-----
 TSLYASNSN--PPKA--LASVTVPNPP--DA--FNSKEGWNTYASGFLIGGIGGAIFAYFLATT--PLLQAFNR-----
 LSLYASNSN--PPKA--LASVTVPNPPVDA--FNSKEGWNTYASGFLIGGIGGAIFAYFLATT--PLLQAFNR-----
 CLSLYASNSN--PAPA--LASVTVPNPPVDA--FNSKEGWNTYASGFLIGGIGGAIFAYFLATT--PLLQAFNR-----
 CLSLYASNSN--PAPA--LASVTVPNPPVDA--FNSKEGWNTYASGFLIGGIGGAIFAYFLATT--PLLQAFNR-----
 ALSLYGSVT-----SQRTNGP-----VKGSQSWSELAAGFLVGGMGGAIFAYFLATT--PLLQAFNR-----
 GLSGYASLV-----EDVP--TE--F--DRKGSRLAGGFLVGGMGGAIFAYFLATT--PLLQAFNR-----



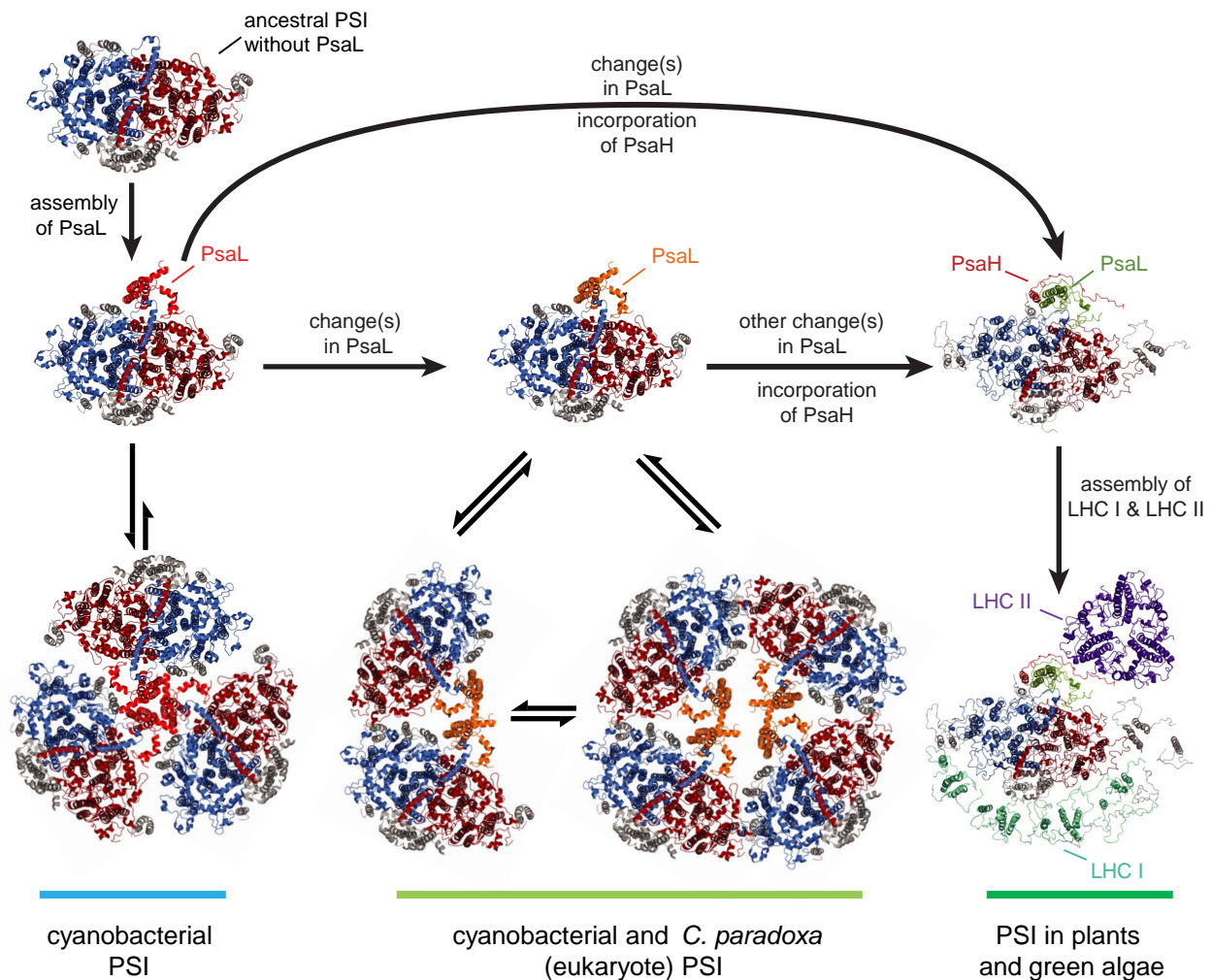
Supplemental Figure 6. Genetic complementation of *Synechocystis* *psaL* using TS-821 *psaL*.

(A) Constructs of *psaL* knockout and complementation. *Synechocystis* *psaL* knockout mutant ($\Delta psal$) was constructed by replacing wild type (WT) *psaL* first 300 bp coding sequence with kanamycin resistant gene (Kan^r). TS-821 *psaL* expressing mutant (CH*psaL*) was constructed by replacing WT *psaL* first 300 bp coding sequence with TS-821 *psaL* and Kan^r open reading frame. NdeI restriction site was created by site directed mutagenesis and used with BstEII to make the constructs. Primers, shown as arrows, binding in WT *psaL* flanking region, at left bound (LB) 500 bp and right bound (RB) 500 bp, were used to identify the transformants.

(B) Identification of homozygous mutants using PCR. Expected fragment sizes of different genetic background are shown in panel (A).

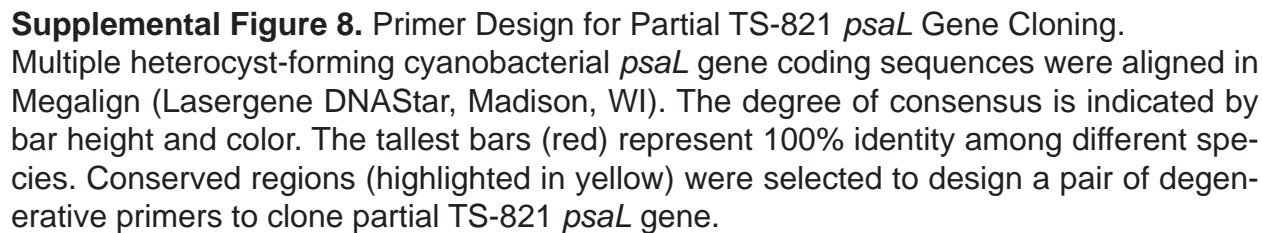
(C) BN-PAGE of solubilized thylakoids of *Synechocystis* WT and mutants. Thylakoids of 0.4mg/mL Chl were solubilized in 1% DDM. PSI trimer and monomer are denoted.

(D) SDS-PAGE of WT PSI trimer and mutants PSI monomers. The band corresponding to PsaL is denoted. Silver stain was used for visualization.



Supplemental Figure 7. Photosystem I Evolutionary Model.

Cyanobacterial PSI was evolved from the ancestral PSI without PsaL. The advent of PsaL in cyanobacteria promotes the trimerization of PSI while the PSI trimer dissociation is not favored. As PsaL evolved with structural modification, PSI trimer becomes less favorable. PSI monomers form dimers and tetramers which in turn dissociate into monomers. This PSI equilibrium is possessed by *C. paradoxa* (eukaryote) as well as cyanobacteria, which indicates the possibility of plastids ancestor has a tetrameric form of PSI. With further PsaL modification and PsaH emergence, the monomeric PSI is exclusively favored in green algae and plants. Alternatively, the monomeric PSI becomes exclusive with one step which involves both PsaL modification and PsaH emergence. Images of PSI and LHC-II are derived from available crystal structures in PDB, 1JB0, 3LW5 and 1RWT.



Multiple heterocyst-forming cyanobacterial *psaL* gene coding sequences were aligned in Megalign (Lasergene DNASTar, Madison, WI). The degree of consensus is indicated by bar height and color. The tallest bars (red) represent 100% identity among different species. Conserved regions (highlighted in yellow) were selected to design a pair of degenerative primers to clone partial TS-821 *psaL* gene.

**Characterization and Evolution of Tetrameric Photosystem I from the Thermophilic
Cyanobacterium *Chroococcidiopsis* sp TS-821**

Meng Li, Dmitry A. Semchonok, Egbert J. Boekema and Barry D. Bruce
Plant Cell; originally published online March 28, 2014;
DOI 10.1105/tpc.113.120782

This information is current as of June 13, 2015

Supplemental Data	http://www.plantcell.org/content/suppl/2014/03/14/tpc.113.120782.DC1.html
Permissions	https://www.copyright.com/ccc/openurl.do?sid=pd_hw1532298X&issn=1532298X&WT.mc_id=pd_hw1532298X
eTOCs	Sign up for eTOCs at: http://www.plantcell.org/cgi/alerts/ctmain
CiteTrack Alerts	Sign up for CiteTrack Alerts at: http://www.plantcell.org/cgi/alerts/ctmain
Subscription Information	Subscription Information for <i>The Plant Cell</i> and <i>Plant Physiology</i> is available at: http://www.aspb.org/publications/subscriptions.cfm